

	<p>Research and Development Programme on Seismic Ground Motion</p> <p>CONFIDENTIAL <i>Restricted to SIGMA scientific partners and members of the consortium, please do not pass around</i></p>	<p>Ref : SIGMA-2013-D1-89 Version : 01</p> <p>Date : Page :</p>
--	--	---



CRUSTAL TOMOGRAPHY 3D vs 1D LOCALIZATION IN THE PYRENEES

(Deliverable D1-89)

AUTHORS			REVIEW			APPROVAL		
NOM	DATE	VISA	NOM	DATE	VISA	NOM	DATE	VISA
T. Theunissen, S. Cheverot, M. Sylvander OMP			J. Douglas BRGM	In written review attached		K. Manchuel		
			M. Granet EOST	In written review attached		G. Senfaute		

DISSEMINATION: Authors; Steering Committee; Work Package leaders, Scientific Committee, Archiving.

	<p style="text-align: center;">Research and Development Programme on Seismic Ground Motion</p> <p style="text-align: center;">CONFIDENTIAL <i>Restricted to SIGMA scientific partners and members of the consortium, please do not pass around</i></p>	<p>Ref : SIGMA-2013-D1-89 Version : 01</p> <p>Date : Page :</p>
--	--	---

DISSEMINATION: Authors; Steering Committee; Work Package leaders, Scientific Committee, Archiving.

Abstract

This work is a part of the work package 1 (WP1) of the SIGMA project entitled *A better knowledge of seismic sources*. Comparisons between 1D and 3D absolute earthquake location processes are led in order to evaluate sensitivity to the numerical representation of P- and S-waves velocity structures. Importance has been given to the geographic reference (plate earth versus ellipsoidal earth) and to the calculation of velocity models that are used by the earthquake location process. Results show us that the fact to take into account the ellipsoidal shape of the earth (vs plate) and the topography is an important issue to estimate together the horizontal position and to improve the hypocenter depth determination. The difficulty is to correctly retrieve a robust 3D velocity model able to improve results obtained with a 1D velocity model. We show that using 3D lateral variations of P- and S-waves velocity fields slightly improve the stability of the absolute earthquake location when the seismic network is small, in particular in depth. Results using a 3D model in Pyrenees are encouraging but some efforts are still necessary to calculate an appropriate 3D velocity model. The dependency to the initial velocity model during 3D inversion and the sensitivity to the S-waves velocity model in the absolute earthquake location process within the 3D a-priori model have to be appraised.

Executive Summary

1) Contributions

The estimation of the absolute earthquake position is an usual and maybe the oldest inverse problem in seismology [Aki et al, 1980]. It is used in routine in all regional seismological observatory through the world in order to build seismicity catalog and/or to realize real-time earthquake location. Usually, HYPO71 software or similar, based on Geiger method [Geiger, 1910], is used. Calculation of synthetic travel-times are realized into a 1D velocity model and static delays can be added to each seismic station in order to account for topography and also sometimes for 3D structures located just beneath the seismic stations. Many researches revealed that the use of a 3D velocity model is an important issue to improve the absolute earthquake location [Flanagan et al., 2007; Font et al., 2004; Simmons et al., 2012; Theunissen et al., 2012]. However, such approaches have been realized at regional and global scale, or also in particular case where events are mainly located far from the first station and associated with an important azimuthal gap, i.e. in network configuration very different that we can find locally. From our knowledge, only few studies have tried to quantify the accuracy of the use of 3D velocity model in comparison of 1D velocity model [Husen et al., 2003] in the optimal seismic network configuration.

Indeed, that is clearly understood in the community that the presence of many seismic stations close and around the seismic event is enough to constrain the hypocenter position [Bondar et al., 2004].

	<p style="text-align: center;">Research and Development Programme on Seismic Ground Motion</p> <p style="text-align: center;">CONFIDENTIAL <i>Restricted to SIGMA scientific partners and members of the consortium, please do not pass around</i></p>	<p>Ref : SIGMA-2013-D1-89 Version : 01</p> <p>Date : Page :</p>
--	--	---

However, we know some evidences that earthquake location can be improved. In complex tectonic contexts as in Alps or Pyrenees where the 3D structure is quite complex the use of many subregional 1D models should be preferred to the use of only one in order to improve the absolute earthquake location [Husen et al., 2011]. Moreover, many local studies have realised 3D earthquake location, for examples see [Satriano et al., 2006; Huang and Zhao, 2012; Mostaccio et al., 2013}, showing that residuals are clearly improved but that the accuracy is not easy to appraise. Comparisons between 3D and 1D show an increase in clustering of seismicity and some clear linear features are also better resolved when using 3D model.

The use of active source (quarry blast, active seismic experiments) as reference are usually used to appraise the accuracy of absolute earthquake locations at this local scale [Husen et al., 1999; Husen et al., 2003; Lin et al., 2006] as well as the quality of 3D velocity models (for example [Satriano et al., 2006; Linet et al., 2011]).

The other main difficulty consists in determine 3D velocity models for P- and S-waves. Many approaches can be used but differences between them are mainly based on the choice of the data that we want to invert and on the choice of the inversion algorithm. Few problems, as for hypocenter determination of shallow events, come from the fact that the shallowest part of the 3D model, beneath seismic stations, is not well constrained.

2) Starting point of the study

Today, Pyrenees are characterized by a low horizontal deformation rate, probably below 0.5 mm/yr [Nocquet et Calais, 2004; Asensio et al., 2012] and by a recurrent seismicity ($M_{\{W\}} < 5$) since the beginning of the previous century. Thanks to the last twenty years of precise monitoring, the spatial distribution of the seismicity is quite well known. To the west, the seismicity is clustered along E-W trending faults with no clear relation to the North Pyrenean fault and more diffuse to the east at the first order [Souriau et Pauchet, 1998, Souriau et al., 2001; Rigo et al., 2005, Ruiz et al., 2006, Lacan et al., 2012]. Major historical earthquakes (with $M_{\{W\}} > 6$ and $M_{\{W\}} \sim 7$) have been identified certainly with a mean recurrence period of a few thousands years. All the Pyrenean seismicity is mainly located in the first 20 km of the crust. Focal solutions of small earthquakes ($M < 4$) determined from the first motions of local or regional P waves are often poorly constrained owing to the bad distribution of stations in azimuth, and show a large variability along the chain [Nicolas et al., 1990; Delouis et al., 1993; Souriau et al., 2001}. Focal mechanisms, estimated from waveforms inversion, evidenced mainly normal faulting [Chevrot et al., 2011] certainly caused by coupling between erosion and isostatic readjustments during last 10 or 20 Ma [Lacan et al., 2012; Vernant et al., 2013] or/and also controlled by rheological contrasts [Souriau et al., 2001; Rigo et al., 2005}. As well as the seismicity and the geology, the relief shows lateral variations from west to east respectively from smooth low relief in the western part to high relief marked by deep valley in the central part to low relief marked by important high plateaus in the east. Among mechanisms responsible of the current neotectonics and geomorphology, deep mechanisms are not well considered in link with the absence a global 3D view of the crustal and lithospheric structure [Gunnell et Calvet, 2006].

For these reasons, it is fair to say that Pyrenean seismicity is still poorly understood. The Pyrenees are thus a perfect example of a region of moderate activity that would benefit from a detailed imaging of crustal structures which would help to improve earthquake locations, identify the active faults, and better quantify seismic hazard.

	<p style="text-align: center;">Research and Development Programme on Seismic Ground Motion</p> <p style="text-align: center;">CONFIDENTIAL <i>Restricted to SIGMA scientific partners and members of the consortium, please do not pass around</i></p>	<p>Ref : SIGMA-2013-D1-89 Version : 01</p> <p>Date : Page :</p>
--	--	---

3) Input Data (nature and origine)

Few bulletins with their picking seismic phases have been combined:

- OMP bulletin for the period 1978/12 - 2011/12 (20561 earthquakes)
- Manual picking from PYROPE and TOPO-IBERIA experiments for the period 2010/09 - 2013/01 (313 earthquakes)
- ReNass bulletin for the period 1987/12 - 2013/02 and CEA bulletin 1978/01 - 2002/31
- Manual picking of accelerometers from RAP (French accelerometric network) and BRGM (French Bureau de Recherches Géologiques et Minières) for the period 2001/05 - 2010/05 (151 earthquakes)
- IGN bulletin (Instituto Geográfico Nacional) for the period 1997/11 - 2013/02 including IGC (Institut Geològic de Catalunya) seismic stations (12469 earthquakes)
- Manual picking from temporary networks of 1996 (336 earthquakes), 1999-2000 and 2001-2002 (361 earthquakes) and 2006 (295 earthquakes). At this moment, dataset from Ruiz et al. [2006] has not been added yet (179 earthquakes)

At final we deal with a catalog of 22762 earthquakes for a total of 440265 phases (235585 P and 204680 S) and, in average, 10.6 ± 8.6 P per event and 8.3 ± 8.5 S per event. 320 seismic stations are used in this dataset.

In addition to these picking information, quarry blasts indexed by the OMP and active seismic experiments [Pedreira et al., 2003] are used to quantify quality of the 3D velocity model and the accuracy of earthquake location.

4) SIGMA Work Package

This work is a part of the work package 1 (WP1) of the SIGMA project entitled *A better knowledge of seismic sources*. As mentioned in the scientific objectives, the two main goals of the WP1 are to produce a catalogue of earthquakes that covers both the historical and instrumental periods, and to improve knowledge of faults and geological structures that are potentially active. This study is a first step to produce, in a near future, a catalog for the Pyrenean seismicity based on 3D absolute earthquake location for which accuracy will be well appraised and in link the Gaussian uncertainties given by the process.

5) Final contribution

At this moment, results show us that the fact to take into account the ellipsoidal shape of the earth (vs plate) and the topography is an important issue to estimate together the horizontal position and to improve the hypocenter depth determination. The difficulty is to correctly retrieve a robust 3D velocity model able to improve results obtained with a 1D velocity model. We show that using 3D lateral variations of P- and S-waves velocity fields slightly improve the stability of the absolute earthquake location when the seismic network is small, in particular in depth. Results using a 3D model in Pyrenees are encouraging but some efforts are still necessary to calculate an appropriate 3D velocity model. The dependency to the initial velocity model during 3D inversion and the sensitivity to the S-waves velocity model in the absolute earthquake location process within the 3D a-priori model have to be appraised.

	<p>Research and Development Programme on Seismic Ground Motion</p> <p>CONFIDENTIAL <i>Restricted to SIGMA scientific partners and members of the consortium, please do not pass around</i></p>	<p>Ref : SIGMA-2013-D1-89 Version : 01</p> <p>Date : Page :</p>
--	--	---

Annexes

Please find in annexe a more complete report with references in the pdf version.

DRAFT

1 Comprehensive 3D absolute earthquakes location
2 (versus 1D) and local seismic tomography of the
3 Pyrenean crust from first arrival times

4 *SIGMA report*

5 T. Theunissen

Observatoire Midi-Pyrénées

IRAP - UMR5277

14, avenue Edouard Belin

31400 Toulouse, France

6 **Abstract**

7
8 This work is a part of the work package 1 (WP1) of the SIGMA project enti-
9 tled *A better knowledge of seismic sources*. Comparisons between 1D and 3D absolute
10 earthquake location processes are led in order to evaluate sensitivity to the numerical
11 representation of P- and S-waves velocity structures. Importance have been given to
12 the geographic reference (plate earth versus ellispoidal earth) and to the calculation of
13 velocity models which are used by the earthquake location process. Results show us
14 that the fact to take into account the ellispoidal shape of the earth (vs plate) and the
15 topography is an important issue to estimate together the horizontal position and to
16 improve the hypocenter depth determination. The difficulty is to correctly retrieved a
17 robust 3D velocity model able to improve results obtained with a 1D velocity model.
18 We show that using 3D lateral variations of P- and S-waves velocity fields slightly im-
19 prove the stability of the absolute earthquake location when the seismic network is
20 small, in particular in depth. Results using a 3D model in Pyrenees are encouraging
21 but some efforts are still necessary to calculate an appropriate 3D velocity model. The
22 dependancy to the intial velocity model during 3D inversion and the sensisitivity to
23 the S-waves velocity model in the absolute earthquake location process within the 3D
24 a-priori model has to be apppraised.

25 **1 Introduction**

26 The estimation of the absolute earthquake position is an usual and maybe the oldest in-
27 verse problem in seismology [Aki and Richards, 1980]. It is used in routine in all regional

1 seismological observatory through the world in order to build seismicity catalog and/or to
2 realize real-time earthquake location. Usually, HYPO71 software or similar, based on Geiger
3 method [Geiger, 1910], is used. Calculation of synthetic travel-times are realized into a 1D
4 velocity model and static delays can be added to each seismic station in order to account for
5 topography and also sometimes for 3D structures located just beneath the seismic stations.
6 Many researchs revealed that the use of a 3D velocity model is an important issue to improve
7 the absolute earthquake location [Flanagan et al., 2007; Font et al., 2004; Simmons et al.,
8 2012; Theunissen et al., 2012]. However, such approaches have been realized at regional
9 and global scale, or also in particular case where events are mainly located far from the
10 first station and associated with an important azimuthal gap, i.e. in network configuration
11 very different that we can find locally. From our knowledge, only few studies have tried to
12 quantify the accuracy of the use of 3D velocity model in comparison of 1D velocity model
13 [Husen et al., 2003] in the optimal seismic network configuration. Indeed, that is clearly
14 understand in the community that the presence of many seismic stations close and around
15 the seismic event are enough to constrain the hypocenter position [Bondar et al., 2004].
16 However, we know some evidences that earthquake location can be improved. In complex
17 tectonic contexts as in Alps or Pyrenees where the 3D structure is quite complex the use of
18 many subregional 1D models should be preferred to the use of only one in order to improve
19 the absolute earthquake location [Husen et al., 2011]. Moreover, many local studies have
20 realised 3D earthquake location, for examples see [Satriano et al., 2006; Huang and Zhao,
21 2012; Mostaccio et al., 2013], showing that residuals are clearly improved but that the accu-
22 racy is not easy to appraise. Comparisons between 3D and 1D show an increase in clustering
23 of seismicity and some clear linear features are also better resolved when using 3D model.
24 The use of active source (quarry blast, active seismic experiments) as reference are usually
25 used to appraise the accuracy of absolute earthquake locations at this local scale [Husen
26 et al., 1999, 2003; Lin et al., 2006] as well as the quality of 3D velocity models (for example
27 [Satriano et al., 2006; Lin et al., 2011]). The other main difficulty consists in determine 3D
28 velocity models for P- and S-waves. Many approachs can be used but differences between
29 them are mainly based on the choice of the data that we want to invert and on the choice of
30 the inversion algorithm. Few problems, as for hypocenter determination of shallow events,
31 come from the fact that the shallowest part of the 3D model, beneath seismic stations, is
32 not well constrained.

33

34 Purpose of this study is to quantify benefits of the 3D absolute earthquake location in
35 the Pyrenean chain in order to consider the creation of a 3D location routine to perform
36 earthquake location in the Pyrenean seismological center (RSSP : Réseau de Surveillance
37 Sismique des Pyrénées). Update of the RSSP seismicity catalog will be also realized. This
38 work consequently needs the building of 3D P- and S- velocity models thanks to seismic
39 tomography. It takes advantages of SISPYR and PYROPE projects for which new seismic

1 stations have been deployed or updated last years.

2 First of all, a short geological context is presented. The second section gives a short
3 description of the entire dataset used in this study. The methodology and the approach
4 are then presented in the following section. Finally, first results are shown and discus-
5 sions/prospectives will come conclude this report.

6 2 Geological context

7 The Pyrenees are a N110° trending mountain range aligned with the Cantabrian Mountain
8 in the northern edge of the Iberian Peninsula. While Cantabrian Mountain is located at the
9 boundary between continental Iberia and oceanic Bay of Biscay to the North, the Pyrenean
10 Mountain is a continental asymmetrical orogenic wedge more developed on its southern side
11 and delimited by two oceanic basins, the Bay of Biscay to the west (Atlantic ocean) and
12 the Golfe of Lion to the East (Mediterranean Sea) (Figure 1). Onshore, two meso-cenozoic
13 basins surround the Pyrenees, the Aquitania Basin to the north and the Ebro Basin to the
14 south. The Pyrenees are the consequence of the collision between the microcontinent Iberia
15 and the southwesternmost part of the Eurasian plate from Upper-cretaceous (85Ma) to Late
16 Oligocene (25Ma) [Fitzgerald et al., 1999].

17 The existence and the size of an oceanic basin before this period, during the Cretaceous,
18 and the total amount of shortening are debated [Visser and Meijer, 2012; Sibuet et al.,
19 2004; Bronner et al., 2011, 2012; Tucholke and Sibuet, 2012] mainly in link with the opening
20 of the Bay of Biscay and displacement of the Iberia. Whatever happened, the cretaceous
21 sedimentary basin was characterized by a very important thinning that later controlled
22 the deformation during the shortening process [Jammes et al., 2010, 2009] and no geological
23 evidences are in agreement with the existence of an oceanic basin. Moreover, only peridotites
24 (Figure 1 - B) with continental signature, in link with the cretaceous thinned margin, are
25 squeezed in the collision zone along the north Pyrenean domain (Figure 1) [Clerc et al.,
26 2012; Jammes et al., 2010, 2009; Bodinier et al., 1988] and visible as well on outcrops as in
27 geophysical observations (Bouguer Anomalies, velocity anomalies) [Granjean, 1994; Souriau
28 and Granet, 1995; Jammes et al., 2010; Clerc et al., 2012; Lagabrielle et al., 2010].

29 The crustal and lithospheric structure of this region has been relatively well imaged from
30 seismic reflexion [Roure et al., 1989; Daignieres et al., 1989; Choukroune, 1990; Senechal and
31 Thouvenot, 1994], seismic refraction [Hirn et al., 1980; Gallart et al., 1980, 1981; Pedreira
32 et al., 2003], gravity modelling [Torre et al., 1989; Vacher and Souriau, 2001; Pedreira et al.,
33 2007; Jammes et al., 2010], local and/or teleseismic seismic waves inversions [Souriau and
34 Granet, 1995; Souriau et al., 2008], receiver functions analysis [Diaz et al., 2012] and magne-
35 totellurics inversions [Pous et al., 1995; Ledo et al., 2000; Campanya et al., 2012]. The Moho
36 has been mapped from a compilation revealing the important and continue crustal root from
37 west to east and an important decrease in the eastern part approaching the Golfe of Lion

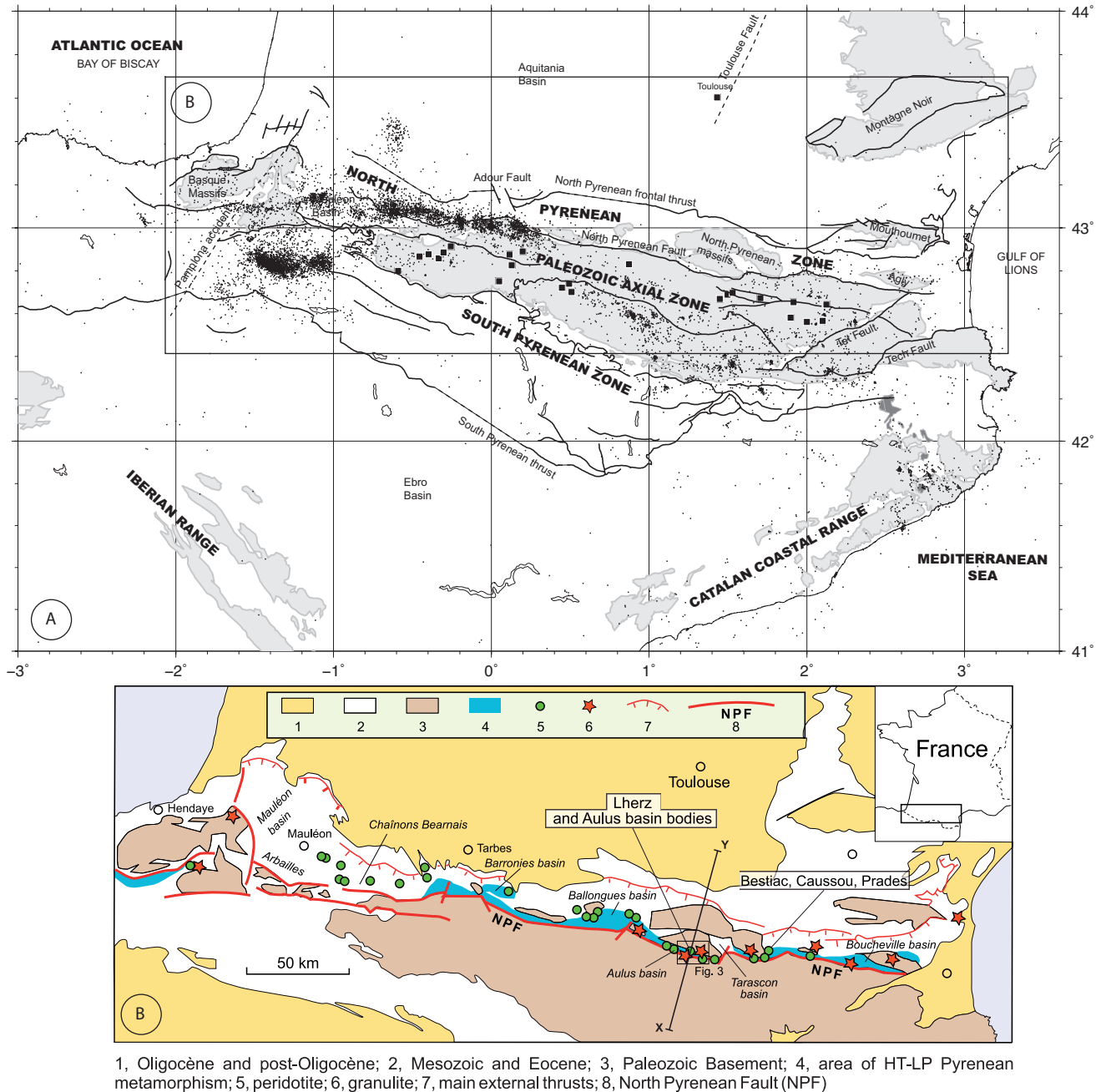


Figure 1: Main structural units of the Pyrenees. A: gray: pre-mesozoic basement, dark-gray: tertiary and quaternary Catalana volcanism, small black dots : seismicity recorded by the OMP since January 2006. B: Simplified geological map of the Pyrenean belt with location of the peridotite bodies in the eastern portion of the belt (from Clerc et al. [2012]).

1 [Diaz and Gallart, 2009]. All these studies reveal the subduction of the Iberia beneath Aquitania and an important thickening of the continental crust, at least down to 55-60 km. This
2 tania and an important thickening of the continental crust, at least down to 55-60 km. This
3 feature seems to continue through the Cantabrian Mountain with important lateral varia-
4 tions regarding the Moho geometry [Diaz and Gallart, 2009; Pedreira et al., 2010]. Several
5 authors suggest that the crustal root in the Pyrenees reach 80-100 km in depth, based on
6 geological balancing of crustal cross sections [Munoz, 1992; Verges et al., 1995; Teixell, 1998],
7 seismic tomography [Souriau and Granet, 1995; Souriau et al., 2008] and magnetotelluric re-
8 sults [Pous et al., 1995; Ledo et al., 2000; Campanya et al., 2012]. To the west, the restoration
9 of the crustal cross section across the Cantabrian Mountains also suggests that some lower
10 crustal material may be subducted into the mantle to depths of 90 km [Gallastegui, 2000].
11 Deeper in the lithosphere, the uncertainties concerning the structure greatly increase.

12 Today, Pyrenees are characterized by a low horizontal deformation rate, probably below
13 0.5 mm/yr [Nocquet and Calais, 2004; Asensio et al., 2012] and by a recurrent seismicity
14 ($M_W < 5$) since the beginning of the previous century. Thanks to the last twenty years
15 of precise monitoring, the spatial distribution of the seismicity is quite well known. To the
16 west, the seismicity is clustered along E-W trending faults with no clear relation to the North
17 Pyrenean fault and more diffuse to the east at the first order [Souriau and Pauchet, 1998;
18 Souriau et al., 2001; Rigo et al., 2005; Ruiz et al., 2006; Lacan and Ortuno, 2012]. Major
19 historical earthquakes (with $M_W > 6$ and < 7) have been identified certainly with a mean
20 recurrence period of a few thousands years. All the Pyrenean seismicity is mainly located in
21 the first 20 km of the crust. Focal solutions of small earthquakes ($M < 4$) determined from
22 the first motions of local or regional P waves are often poorly constrained owing to the bad
23 distribution of stations in azimuth, and show a large variability along the chain [Nicolas
24 et al., 1990; Delouis et al., 1993; Souriau et al., 2001]. Focal mechanisms, estimated from
25 waveforms inversion, evidenced mainly normal faulting [Chevrot et al., 2011] certainly caused
26 by coupling between erosion and isostatic readjustments during last 10 or 20 Ma [Lacan and
27 Ortuno, 2012; Vernant et al., 2013] or/and also controlled by rheological contrasts [Souriau
28 et al., 2001; Rigo et al., 2005]. As well as the seismicity and the geology, the relief shows
29 lateral variations from west to east respectively from smooth low relief in the western part
30 to high relief marked by deep valley in the central part to low relief marked by important
31 high plateaus in the east. Among mechanisms responsible of the current neotectonics and
32 geomorphology, deep mechanisms are not well considered in link with the absence a global
33 3D view of the crustal and lithospheric structure [Gunnell and Calvet, 2006]. For all these
34 reasons, it is fair to say that Pyrenean seismicity is still poorly understood. The Pyrenees
35 are thus a perfect example of a region of moderate activity that would benefit from a detailed
36 imaging of crustal structures which would help to improve earthquake locations, identify the
37 active faults, and better quantify seismic hazard.

3 Data

This study combines all available picking data for the period 1978-2013 (Figure 2). The two first subsections describe the evolution of the seismic network through the time together with the description of temporary seismic networks deployed in the study area. The third subsection describes the data selection used in this study.

Seismic monitoring in the Pyrenees: a quick review

Reader may refer to Souriau et Granet [1995], Souriau et Pauchet [1998] and Souriau et al. [2001] for more details about the seismic monitoring evolution in Pyrenees since 1960. Before this date no seismometer were installed. Only few seismic stations were running between 1960 and 1978 (Astronomical Observatory of the Pic du midi, MLS (IPGP) and EPF (LDG/CEA)). After the moderate-size M_W 5.0 1967 Arette earthquake in the west of the Pyrenees [Cara et al., 2008], the IPGP (Institut de Physique du Globe de Paris) has installed, between 1976 and 1983, about nine short-period seismic stations in the west part of the Pyrenees becoming permanent stations with radio transmission of the data. This “Arette” network was running until 1992. In 1988-89, 10 permanent short-period seismic stations have been deployed in the eastern and central part of the Pyrenees and data were transmitted through the Meteosat satellite to the Observatoire Midi-Pyrenees (OMP) and then to the national seismological center, the Réseau National de Surveillance Sismique (ReNaSS). At the same moment, a dense network of about 10 stations existing for a field survey at Lacq was running [Souriau and Pauchet, 1998]. From 1997 up today, the OMP network was re-deployed over the whole Pyrenees with three components short-period seismometers with data transmission by telephone and recording data after STA/LTA launching. Since SISPYR, SIHEX and RESIF projects, broadband seismic stations have been deployed at new place or updated at some old place. Few temporary seismic networks have been also deployed during the last thirty years, in particular:

- **1996:** 30 short-period seismic stations with 3 or 1 component during 6 days around the Agly massif following the Saint-Paul-de-Fenouillet earthquake ($M_L = 5.2$) [Pauchet et al., 1999]
- **1999-2000 and 2001-2002:** 5 short-period stations with vertical component during 6 months in 1999-2000 and 10 short-period instruments with three components during 6 months in 2001-2002 in the neighbourhood of the Adour fault near Lourdes [Dubos et al., 2004]
- **2006:** 6 short-period instruments with three components during two months in the same place following the Argelès-Gazost earthquake ($M_L = 5.0$) [Sylvander et al., 2008]

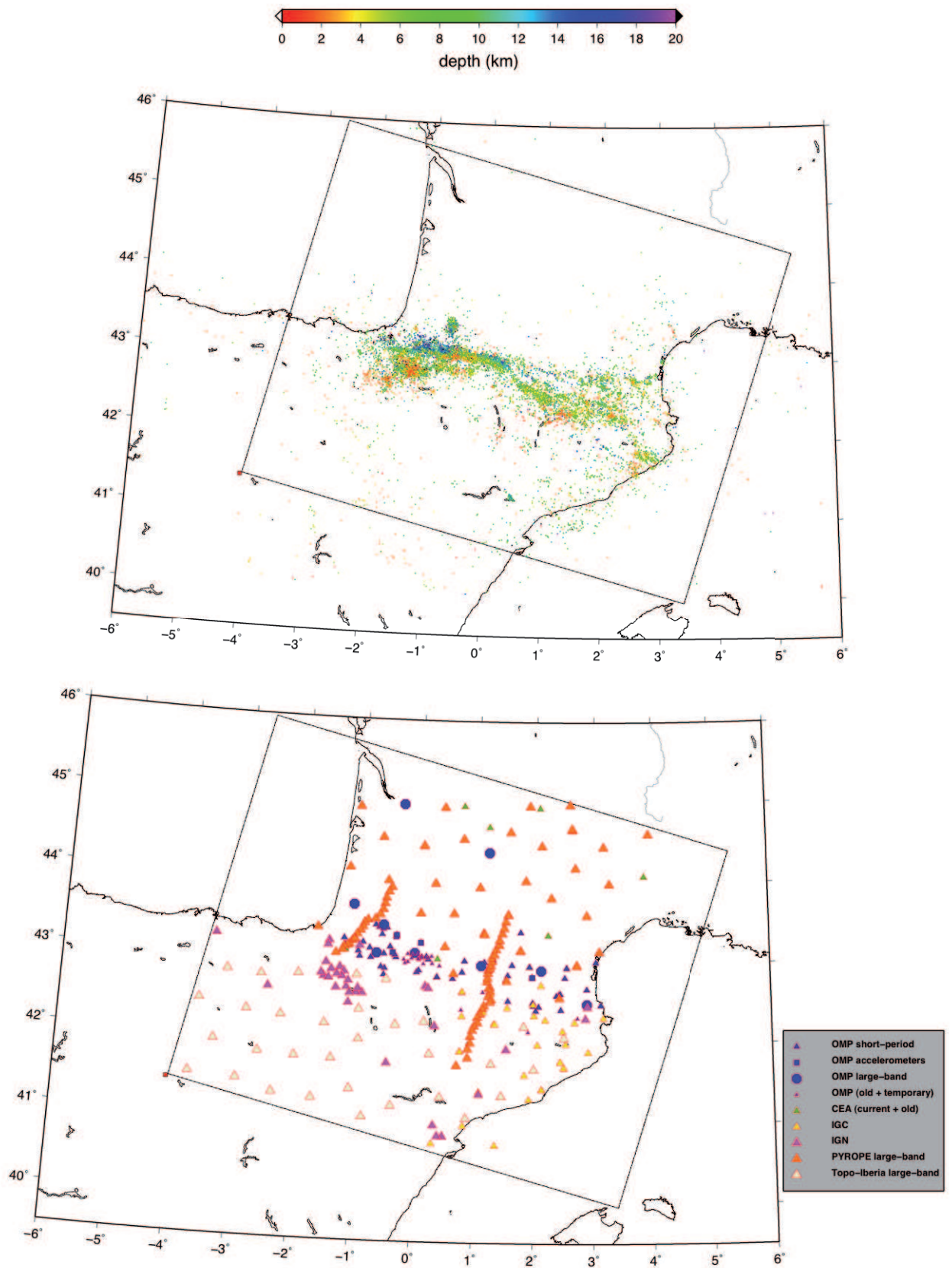


Figure 2: Up: Seismicity compilation for the period 1978/12 - 2013/01. 22762 earthquakes with in average, 10.6 ± 8.6 P per event and 8.3 ± 8.5 S per event. Down: 320 seismic stations of the compilation.

- 1 • **1999-2000:** 11 temporary seismic stations in the westernmost part of the Pyrenees
 2 in two phases (6 months from March 1999 and 9 months from September 2000) [Ruiz
 3 et al., 2006].

4 *PYROPE and TOPO-IBERIA experiments*

5 The PYROPE passive seismic experiment have led to the deployment of a transportable
 6 array of broadband stations with a regular spacing of about 60 km in the same time period
 7 as the third leg of the TOPO-IBERIA experiment in Spain (autumn 2010 to autumn 2012).
 8 This broadband array has been complemented by two 6-month 2D N-S transects (medium
 9 band sensors) across key geological/geodynamical targets, to the east at the same place than
 10 the Pyrenees ECORS profile from June 2012 and to the west through the Mauleon Basin
 11 from December 2012.

12 *Quarry blasts*

13 The RSSP has identified and indexed about 2000 quarry blasts recorded between 1997 and
 14 2011. These blasts have been recorded in average by 3.6 ± 2.1 seismic stations. Only few
 15 blasts have been located with a relative well accuracy in link with the low azimuthal coverage
 16 and the quite large distance to the first station. That is one of the reason that explains that
 17 this dataset has never been exploited yet.

19 *Dataset*

20 Few bulletins with their picking seismic phases have been combined (Figure 2):

- 21 • OMP bulletin for the period 1978/12 - 2011/12 (20561 earthquakes)
- 22 • Manual picking from PYROPE and TOPO-IBERIA experiments for the period 2010/09
 23 - 2013/01 (313 earthquakes)
- 24 • ReNass bulletin for the period 1987/12 - 2013/02 and CEA bulletin 1978/01 - 2002/31
- 25 • Manual picking of accelerometers from RAP (French accelerometric network) and
 26 BRGM (French Bureau de Recherches Géologiques et Minières) for the period 2001/05
 27 - 2010/05 (151 earthquakes)
- 28 • IGN bulletin (Instituto Geográfico Nacional) for the period 1997/11 - 2013/02 including
 29 IGC (Institut Geològic de Catalunya) seismic stations (12469 earthquakes)
- 30 • Manual picking from temporary networks of 1996 (336 earthquakes), 1999-2000 and
 31 2001-2002 (361 earthquakes) and 2006 (295 earthquakes). At this moment, dataset
 32 from Ruiz et al. [2006] has not been added yet (179 earthquakes)

1 At final we deal with a catalog of 22762 earthquakes for a total of 440265 phases (235585
2 P and 204680 S) and, in average, 10.6 ± 8.6 P per event and 8.3 ± 8.5 S per event. 320
3 seismic stations are used in this dataset.

4 Methodology

5 *General demarche*

6 Purpose is to obtain precise absolute P and S –waves velocity fields within the Pyrenean
7 mountain and the best seismicity location. To do this, first arrivals times recorded by per-
8 manent and temporary seismic stations since 1978 are used. After obtaining the best earth-
9 quake location for the entire seismicity and the associated 3D upper crust velocity model,
10 the lower-crust have been imaged using refracted phases. This work is then divided into few
11 successive steps: (i) Initial velocity models determination: Inversion of a 1D minimum model
12 and associated stations delays, building of 3D a-priori velocity models (ii) 3D earthquake
13 location within initial a-priori velocity models using stations delays (1D minimum velocity
14 models and other 3D a-priori models) (iii) 3D local seismic tomography using only P_G and
15 S_G phases and final earthquake location (iv) 3D local tomography using all direct and re-
16 fracted first arrivals phases combining 3D a-priori models including results from upper crust
17 seismic tomography, information about Moho and final 3D earthquake location

18 *Geographic reference*

19 Earthquake location and 3D seismic tomographic algorithms use a 3D regularly spaced par-
20 allelepiped grid to calculate travel-time tables. In such situation, calculations are realised
21 in cartesian coordinates. Two different approximations are then used and compared in this
22 study: plate and ellipsoidal earth approximations. The geodetic coordinate conversions al-
23 lows in both case to obtain Cartesian coordinates (in km) from geodetic coordinate based
24 on the WGS-84 geographic referential. The first one is based on Lambert III ‘s cylindrical
25 equal area (France – IGN) projection except that origin is arbitrary (here, Origin: 41.4°N
26 -4.1°E). In this system, there are only few centimetres of difference with the Universal Trans-
27 verse Mercator projection. The second one uses the Geocentric referential. To do so we use
28 equations based on the tangent of the latitude for both side conversion. After conversion,
29 Cartesian coordinates are rotated and translated in order to be commonly North-South
30 oriented with an (0,0,0) origin. Reader may refer to Bomford [1980] or Featherstone and
31 Claessens [2008] for equations.

1 *Determination of initial velocity models*

2 The important point in such study is to correctly consider the coupled hypocenter velocity
 3 problem [Crosson, 1976]. Biases originating from 3D structure are responsible of correlated
 4 travel-times estimation errors in earthquake location [Chang et al., 1983; Myers and Schultz,
 5 2000; Bondar and McLaughlin, 2009] and non-linear features [Thurber, 1992; Eberhart-
 6 Phillips and Michael, 1993; KISSLING et al., 1995]. To avoid such phenomena, 3D a-
 7 priori velocity models can provide first order of lateral variations as slab plunging, oceanic
 8 crust versus continental crust, sedimentary basins and Moho depth variations [Flanagan
 9 et al., 2007; Font et al., 2004, 2013]. As for the use of 1D model [Kissling, 1988; Kissling
 10 et al., 1994; Flanagan et al., 2007], a static delay (station correction) applied to travel-times
 11 estimations at each seismic station allows improving the earthquake location [Font et al.,
 12 2004]. The station correction takes into account reproducible travel-times misestimation
 13 due to a particular velocity field located under the seismic station. The station correction
 14 can be estimate by joint inversion for 1D model [Kissling, 1988; Pujol, 1988, 2000] or also by
 15 an approximate technique [Frohlich, 1979] that consists in doing the average of the arrival
 16 time residuals for each station and for all the events (valuable with large dataset [Pujol,
 17 1988]). In this work we decide to test earthquake location with few a-priori velocity models
 18 (1D minimum model and few 3D a-priori models) using station corrections and to test the
 19 3D seismic tomography sensitivity to the initial velocity model. Station corrections are only
 20 used for earthquake location purpose.

21 *Minimum 1D model and associated stations delays*

22 Following a usual approach, we built a minimum 1D velocity model thanks to the VELEST
 23 3.1 program [Kissling, 1988; Kissling et al., 1994; KISSLING et al., 1995]. This program
 24 has originally been developed to derive a well-suited initial reference velocity model for 3D
 25 local earthquake tomography [Kissling et al., 1994]. It may also be applied to joint hypocen-
 26 ter determination problem in order to take into account coupling between hypocentral and
 27 velocity parameters [Thurber, 1992]. Here, we performed a combined inversion of veloc-
 28 ity model, source parameters (position and origin time) and station delays using P and S
 29 arrival-times provided by a selected dataset (2051 earthquakes with at least 12 P and 6 S
 30 phase observations with azimuthal gap $< 180^\circ$). A trial-and-error process is led by repeating
 31 this inversion with few initial velocity models (derived from the OMP observatory routine
 32 1D model and the 1D model from Souriau and Granet [1995] and hypocentral parameters
 33 (from OMP bulletins), and for different damping values in order to obtain the so-called best
 34 Minimum 1D velocity model (Figure 3).

35
 36 As for the next 3D demarche, P_G and S_G are first used to determine jointly the upper-
 37 layers velocity field with hypocenters position and stations corrections. Then refracted phases

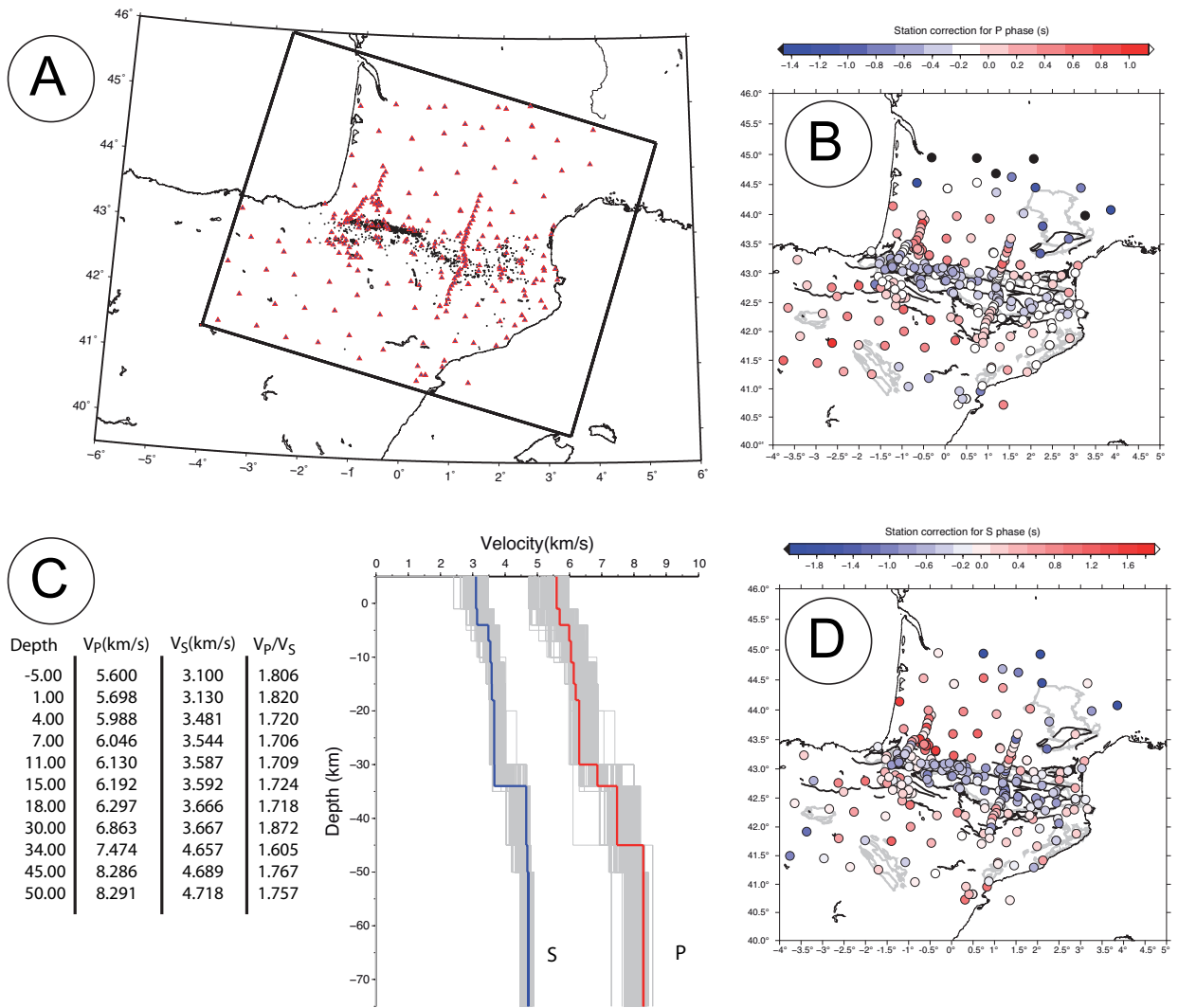


Figure 3: 1D minimum velocity model and associated station delays. A: 2051 earthquakes used in the 1D joint inversion with at least 12 P and 6 S phase observations with azimuthal gap $< 180^\circ$. B: P station delays. C: 1D P- and S-waves velocities and D: S station delays.

1 are added in order to describe lower-layers and determine station corrections for further
 2 seismic stations by damping upper-layers and hypocenters position previously estimated.
 3 Station corrections of closest seismic stations well describe straightforward shallow geological
 4 observations (basement and meso-cenozoic sedimentary basins) while that of further seismic
 5 stations, north of the Aquitania basin and South-west of the Ebro basin, contain information
 6 about Moho depth, mantel velocities and error associated with plate earth approximation
 7 (Figure 3). As previously mentioned, we may remark some discrepancies associated with few
 8 Pyrope temporary seismic stations having clock problem (Figure 3).

9 *Building of a 3D a-priori model and associated stations delays*

10 3D a-priori models are built through the combination of many consecutives 2D lines equally
 11 distanced depending of the inversion grid size. Work consists, first, in the realisation of 2D
 12 map of four interfaces (Figure 4):

- 13 • **Relief** topography and bathymetry come from ETOPO with 1 minute resolution
 14 (about 1.5 km) [Amante and Eakins, 2009]
- 15 • **Basement top** that corresponds to the bottom of Meso-Cenozoic Ebro and Aquitania
 16 basins. Data come from a compilation from isobaths maps and well data.
- 17 • **Lower crust limit** This limit is quite well visible on few refraction 2D lines west of the
 18 Pyrenees [Pedreira et al., 2003]. An average lower crust interface is also given within
 19 the Eucrust-07 model [Tesauro et al., 2008]. However, we choose to use a smooth
 20 velocity field through the crust in order to avoid as far as possible any kind of body
 21 waves complications as refracted waves within the crust and also because this last is
 22 not well constrained over the entire region.
- 23 • **Mohorovicic topographies of Iberia and Eurasia crusts** We made a compilation
 24 from Pedreira et al. [2007]; Diaz and Gallart [2009]; Diaz et al. [2012] and receiver
 25 function calculation at PYROPE, TOPO-IBERIA and RLBP seismic stations (Réseau
 26 Large Bande Permanent) [Chevrot, 2013, personal communication]

27 Secondly, we choose initial P- and S- waves velocity fields applied between interfaces.
 28 Few methods could be considered to obtain such information. We could just attribute
 29 velocities along each interfaces and calculating velocity field by linear interpolation between
 30 each interfaces as in the forward refraction approach. However, refraction 2D lines are
 31 not enough to constrain such interface velocities and too much unknowns interface should
 32 be considered. We could also decide to apply constant mean velocity based on previous
 33 compilation as Eucrust-07. However, as mentioned previously, we do not use lower crust
 34 interface in our model as the one described in Eucrust-07. We rather decide to apply a
 35 smooth gradient fitting average features of the crustal velocity field within the basement

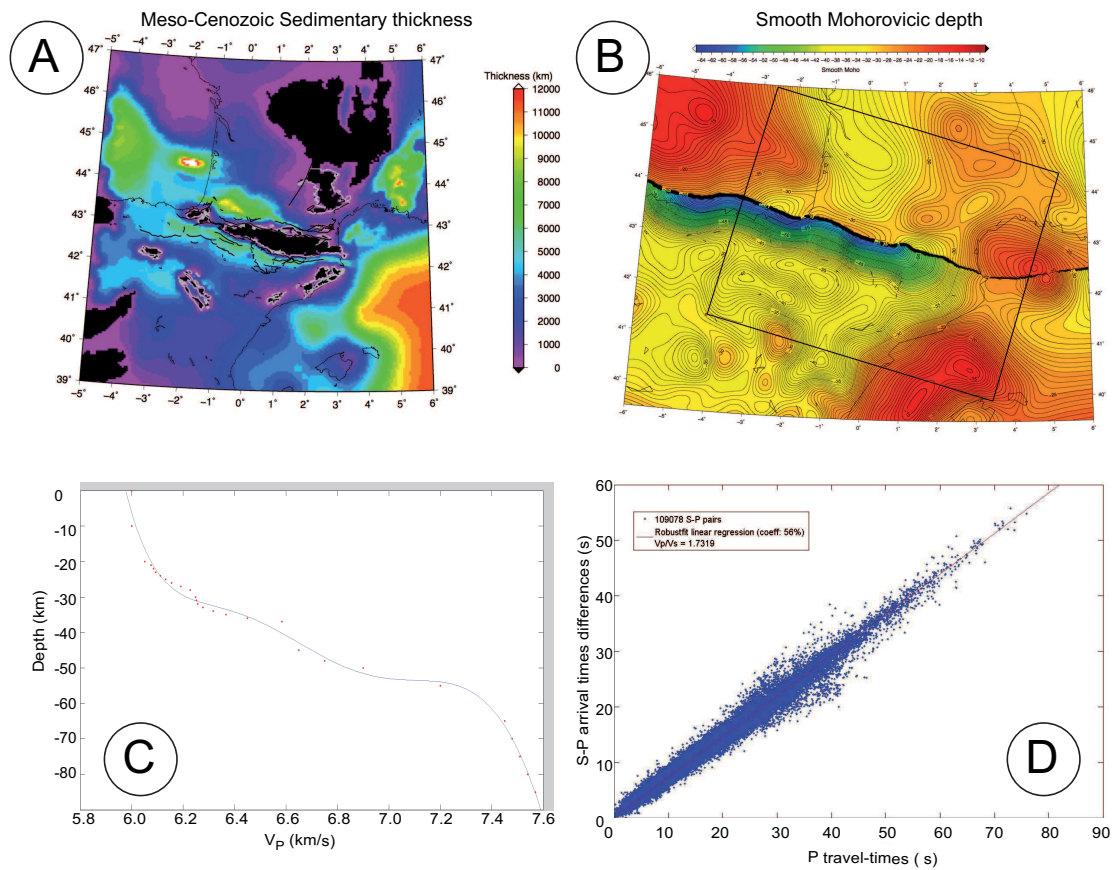


Figure 4: Geological and geophysical inputs for the 3D a-priori velocity model. A: Thickness of Ebro and Aquitania sedimentary basins. B: Smooth Mohorovicic discontinuity built from compilation of Pedreira et al. [2007]; Diaz and Gallart [2009]; Diaz et al. [2012] and receiver function calculation at PYROPE, TOPO-IBERIA and RLBP (Réseau Large Bande Permanent) [Chevrot, 2013, personal communication]. C: smooth gradient used for VP within the basement (i.e., the crust minus sedimentary basins). D: Wadati diagram for a selection of about 11000 well located earthquakes within the 1D minimum velocity model with station delays into the Plate earth approximation.

1 in opposite to the sedimentary basin for which we applied a constant average velocity of
 2 5.0 km/s for P-waves velocity (Figure 5). For S-waves, we apply a constant V_P/V_S ratio.
 3 The Wadati diagram, based a dataset of well-located earthquake determined within the 1D
 4 minimum velocity model with station corrections, gives a mean V_P/V_S ratio of 1.732 ± 0.032 .
 5 After preliminary inversions, we apply a V_P/V_S ratio of 1.76 within the basin and 1.73 within
 6 the basement.

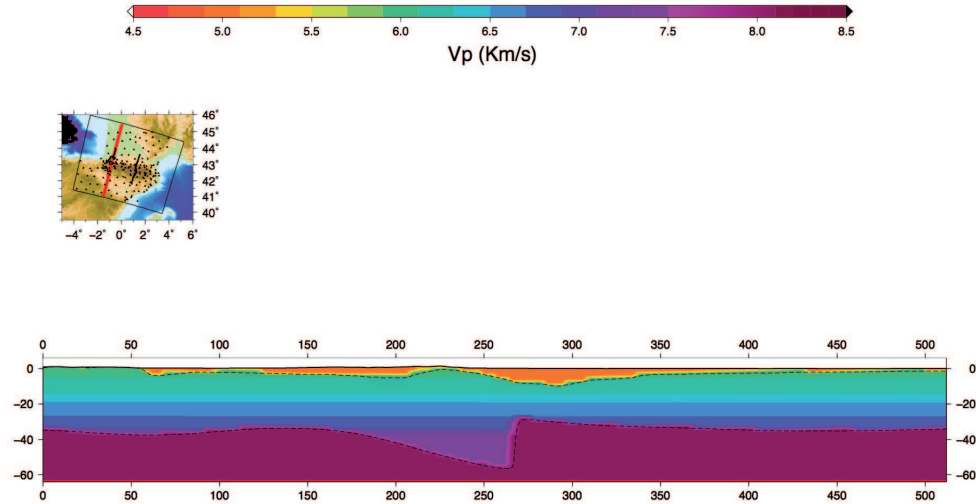


Figure 5: Vertical cross-section through the 3D P-waves velocity model.

7 At final, we have 4 velocity models summarized here after :

- 8 • the Minimum 1D model both with the Plate and the Ellipsoidal earth approximation
 9 : used for earthquake location purpose
- 10 • the P-Minimum 1D model + constant V_P/V_S ratio of 1.73 + a Moho at 35 km depth
 11 : used for initial velocity model in tomography
- 12 • the P-Minimum 1D model + constant V_P/V_S ratio of 1.73 + a 2D smooth Moho similar
 13 to the 3D a-priori model : used for initial velocity model in tomography
- 14 • the 3D a-priori model with the Ellipsoidal earth approximation : : used for earthquake
 15 location purpose and for initial velocity model in tomography

16 *3D Earthquake location*

17 Bondar and McLaughlin [2009] propose to use a linearized iterative location algorithm tak-
 18 ing into account the correlated travel-times errors associated with heterogeneities located
 19 between stations and hypocenter which are not considered within the velocity model and
 20 station correction. We rather decide here to use the NLLoc software (NonLinLoc [Lomax
 21 et al., 2000]) for three reasons (1) the solution can be described by a probability density func-
 22 tion (pdf) (i.e Tarantola and Valette [1982], Moser et al. [1992] and Wittlinger et al. [1993])

1 based on EDT (Equal Differential Time) [Zhou, 1994; Font et al., 2004; Lomax, 2005], (2)
 2 the weighting scheme is well designed and (3) the search algorithm, called Octree, is efficient
 3 and allows to well browse the entire structure leading also to a well estimate of the location
 4 pdf. The concept of EDT allows to better avoid eventual outliers and to be independent of
 5 the origin time [Font et al., 2004; Theunissen et al., 2012]. The weighting scheme of NLLoc
 6 allows considering Gaussian modelisation-error covariances between all station-pairs, using
 7 a station-distance weighting to each travel-times and adding a weight for each station that
 8 is a function of the average distance between all stations used for location that helps to
 9 correct for irregular station distribution and limits correlated travel-times errors. At last
 10 since purpose is also to use 3D models from inversion, NLLoc is then perfectly adapted to
 11 our study. Travel-times tables' calculation is based on the Eikonal propagation equation and
 12 is processed with a finite difference algorithm [Podvin and Lecomte, 1991].

13 In order to validate results from various 3D absolute earthquake location processing, we
 14 use a selection of events that are used as reference. We selected, first, events located by
 15 temporary networks and thus well recorded at short distance and with small azimuthal gap
 16 and consequently associated with a good accuracy according to network criteria [Bondar
 17 et al., 2004] and, second, quarry blasts for which position are known (Figure 6). Three
 18 selected quarry blasts recorded on each side of the Pyrenees allows us to quantify accuracy
 19 on the hypocenter determination using different velocity models (few initial + final velocity
 20 models) using or not stations corrections. Three sequences of seismic events have been well
 21 studied in the past using temporary seismic stations:

- 22 1. the Argelès aftershocks sequence following the Argelès-Gazost earthquake ($M_L = 5.0$)
 23 from 2006 November 17 to the end of December. Aftershocks, relocated in a 3D velocity
 24 model, are well distributed along an E-W trending normal fault [Sylvander et al., 2008].
- 25 2. the Cauterets sequence following two moderate earthquakes ($M_L = 4.6$ and 4.3) be-
 26 tween 2002 May, 16 and 2002 May, 20 is distributed in two very clustered small swarms
 27 that have been relocated by double-difference relative location process [Dubos et al.,
 28 2004].
- 29 3. The Agly sequence from 1996 February, 18 to February, 24 following the Saint-Paul-
 30 de-Fenouillet earthquake ($M_L = 5.2$) [Rigo et al., 1997; Pauchet et al., 1999; Sylvander
 31 et al., 2007] in the east side of the Pyrenees

32 These seismic sequences are used to test:

- 33 1. the clustering of seismicity by the absolute earthquake location process
- 34 2. network criteria depending of the velocity model

35 The first test is evaluated by statistics according to the barycentre (well valuable for
 36 Cauterets and Agly sequences), visually by mapping seismicity on maps and vertical cross-
 37 sections and at last, by comparisons with results from bibliography. The second test is

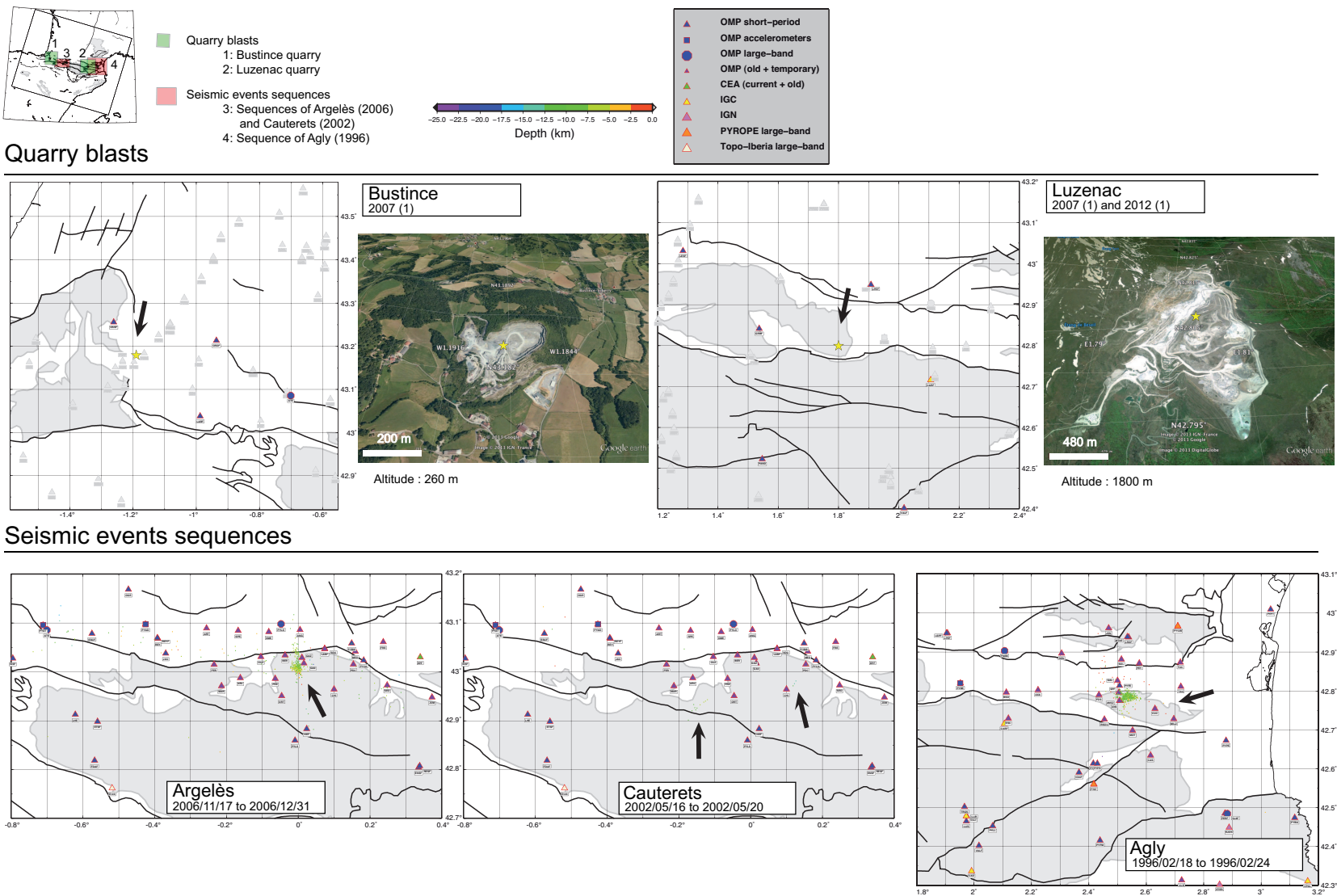


Figure 6: Seismic events used as references. Up: Three quarry blasts. Down: Three seismic sequence for which temporary seismic stations have been deployed.

1 realised only on a selection of three earthquakes, one by seismic sequence, for which network
 2 criteria and quality parameters from location process are good. This test consists by changing
 3 the number of seismic stations used in the process. It is evaluated by the distance with the
 4 optimal solution that is determined with the maximum number of available data. Purpose
 5 of this second test is to quantify the capacity to correctly recover the hypocenter parameters
 6 according to the velocity model (with or not station corrections) function of the number
 7 of seismic stations, the azimuthal gap and the distance to the first station. This aspect
 8 is important within the framework of a seismology observatory for which the earthquake
 9 location depends of the magnitude, i.e. the number of seismic stations recording the event,
 10 and the seismic network geometry. The final 3D velocity model should show the more stable
 11 results (closest of the optimal solution) independently of the number of seismic stations and
 12 network geometry.

13 *3D delayed travel-time tomography*

14 We use a delayed travel-time tomography method to invert simultaneously the velocity dis-
 15 tribution and the hypocenter parameters based on the first arrival-times [Aki and Lee, 1976;
 16 Spencer and Gubbins, 1980; Spakman and Nolet, 1988; Thurber, 1992; Benz et al., 1996].
 17 The code has been developed by Monteiller [2005] and applied in few contexts [Latorre
 18 et al., 2004; Vanorio et al., 2005; Gautier et al., 2006; Theunissen et al., 2012]. The algo-
 19 rithm is based on a-priori assumptions (initial velocity models, earthquake positions and
 20 origin times) from which small perturbations are calculated. The problem becomes linear
 21 (equation 1). This last is used iteratively according to the result of the previous iteration
 22 until the convergence is reached.

$$\delta t = \int_{source0}^{station0} \delta u(x, y, z) dl. \quad (1)$$

23 where the travel-time residual δt is minimized by considering small perturbations δu
 24 of the slowness field u according to the initial models annotated 0 along the ray path l .
 25 The model space is discretised by regular small cube and the linear problem is then posed
 26 according to equation 2.

$$\delta t(source, station) = \sum_{cube} \frac{\delta t}{\delta u} \delta u_{i,j,k} \iff \begin{bmatrix} \frac{\delta t_1}{\delta u_1} & \dots & \frac{\delta t_1}{\delta u_m} \\ \dots & \dots & \dots \\ \frac{\delta t_n}{\delta u_1} & \dots & \frac{\delta t_n}{\delta u_m} \end{bmatrix} = \begin{bmatrix} \delta t_1 \\ \dots \\ \delta t_n \end{bmatrix} \iff A.x = b \quad (2)$$

27 where u is the slowness, n the number of input data (number of rows) and m the number
 28 of unknowns (number of columns), i.e. the number of cells within model by 2 (uP and
 29 uV) and the number of earthquakes by 4 (position coordinates x , y , z and origin time t_0).
 30 The forward problem, to calculate travel-times residuals and to estimative slowness partial

1 derivatives, is based on the Eikonal propagation equation and is processed with a finite
 2 difference algorithm [Podvin and Lecomte, 1991]. A posteriori ray tracing is performed by
 3 computing the travel-time field gradient, and travel time derivatives as well as more accurate
 4 travel times are then calculated [Monteiller et al., 2005]. After modifying variables, V_P and
 5 V_P/V_S are inverted rather than slowness (equation 3).

$$\left\{ \begin{array}{l} dt_S = \frac{\delta t_S}{\delta \frac{1}{V_S}} \cdot \frac{-v}{u^2} du + \frac{\delta t_S}{\delta \frac{1}{V_S}} \cdot \frac{1}{u} dv \\ dt_P = \frac{\delta t_P}{\delta \frac{1}{V_P}} \cdot \frac{-1}{u^2} du \end{array} \right. \quad \text{with} \quad \left\{ \begin{array}{l} u = V_P \\ v = \frac{V_P}{V_S} \end{array} \right. \quad (3)$$

6 The regularisation of the problem is realised by using a diagonal weighting matrix (D1),
 7 a diagonal normalisation matrix (D2), a three directions Laplacian smoothing matrix (L)
 8 and a diagonal damping matrix (DP) according to the following scheme:

$$\begin{pmatrix} D_1 \cdot A \cdot D_2 \\ L \\ DP \end{pmatrix} \cdot y = \begin{pmatrix} D_1 \cdot b \\ 0 \\ 0 \end{pmatrix} \iff A_R \cdot y = b_R \quad (4)$$

9 As proposed by some authors (Le Meur et al., 1997; Spakman and Nolet, 1988), nor-
 10 malization and scaling (through vector D2) of the derivative matrix is performed for better
 11 reconstruction of the different parameters. This operation will remove influences of pa-
 12 rameter units and also will take into account the sensitivity of the data to each class of
 13 parameters. The inverse problem is realised by the LSQR algorithm (Paige and Saunders,
 14 1982) by minimising the norm r (equation 5) according to the small perturbations vector y .

$$r = \left\| A_R \cdot y - b_R \right\|^2 \quad (5)$$

15 The parameters used for the regularization (weighting, smoothing and damping) are not
 16 dimensioned and consequently without units. The weighting is defined by three parame-
 17 ters: phase picking quality, extreme residues and length of rays. The smoothing is defined
 18 for three space directions (x, y and z) and a different coefficient can be applied to V_P and
 19 V_P/V_S . Finally, the damping parameter could be also adjusted for each parameter. All
 20 these parameters are fixed during the inversion and are defined after multiples tests in or-
 21 der obtaining the best compromise between variance reduction, smoothing and amplitude
 22 anomalies.

23 *Grid size and parameterization description*

24 Forward problem:

25 Same travel-times tables, calculated by the Podvin and Lecomte [1991] algorithm, are used
 26 both by the earthquake location code and the tomography code. Only difference is that

1 travel-times tables are not written on hard disk during process but only used to calculate
 2 the travel-time field gradient in the tomography code. For both, we use a cubic cell grid : 1
 3 km x 1 km x 1 km .

4

5 NLLoc parameterization:

6 We use the efficient weights EDT-sum probabilities by the variance of origin-time estimates
 7 over all pairs of readings. This last uses simple statistical estimate of the origin time. All
 8 stations having an epicentral distance higher than 120 km are not used in the earthquake
 9 location process. The weighting calculation to correct for irregular station distribution is
 10 done only with all stations located within 120 km epicentral distance. The search is realised
 11 within the entire model, i.e. a domain of 609 km x 517 km x 79 km. The Octree search is
 12 led by starting with cell sizes of $609/5 \sim 122$ km x $517/5 \sim 104$ km x $79/3 \sim 26$ km. A
 13 solution is given when the minimum cell size of 30 m is reached or if the number of browsed
 14 cells reaches 200000. In one side, we do not use any gaussian modelisation-error covariances
 15 because that is quite impossible to estimate a typical error in seconds for travel-time to one
 16 station due to model errors. In the other side, we set the travel-time error in proportion
 17 to the travel-time, 5% with a minimum of 0.05s and a maximum of 2.0s, in link with the
 18 modelisation-error. At last, we fix the weighting scheme in seconds for phase pick qualities.
 19 We choose 0.05 s, 0.2 s, 0.3 s, 0.5 s and 4.0 s respectively for qualities of 0,1,2,3,4. The solu-
 20 tion is very sensitive to the complete weighting scheme in NLLoc in particular the weighting
 21 due to phase picks quality.

22

23 Inverse problem conditioning:

24 The conditioning of the inversion has been defined after multiples tests for which results
 25 in term of variance reduction and visual aspects were discriminating. We use an inversion
 26 grid cell of 4 km x 4 km x 2 km. This size is a compromise between forward calculation
 27 duration (despite of the fact the code is parallelized) and maximum expected resolution. We
 28 use a Laplacian smoothing $lx.lap(x) + ly.lap(y) + lz.lap(z) = 0$ (matrix L in equation 4) to
 29 limit localized anomalies due to ray theory. For the central part of the inversion box (along
 30 the pyrenean belt up to 40 km depth), smoothing coefficients (lx,ly,lz) are 2x2x0.5 and the
 31 double outside. We use the same damping value 0.9 for all parameters ($V_P, V_S, position$ and
 32 t_0) during the inversion (matrix DP in equation 4). We define scaling coefficients for all
 33 parameters which are inverted : 1 for V_P , 2 for V_P/V_S , 0 for positions and 5 for t_0 . This
 34 scaling means that positions are not inverted during process and that the origin time is free
 35 to change according to others parameters. When refracted phases (P_n and S_n) are used in
 36 the process, rather than only P_G and S_G phases, damping is 1 and scaling scheme is 1 for
 37 V_P , 2 for V_P/V_S , 0 for positions and 0 for t_0 .

38

39 Approximations:

1 The smoothing is realised within a Cartesian inversion grid. Consequently it cuts the ellip-
 2 soidal earth interlinked with the Cartesian grid. The center of the geocentric conversion is
 3 located at the center of the Pyrenees (42.8°N-0.6°E close to the Aneto culminating at 3404
 4 m), within the target area. The ellipsoidal approximation is quite negligible at this place
 5 and the effect of such approximation is also quite negligible. The interest of such approx-
 6 imation is to correctly describe Pn and Sn rays paths even if smoothing effect outside the
 7 target area is quite inadapted but have no major effect on results.

8 A sphere within a cubic grid is quite inadapted because interfaces are quite bad resolved.
 9 According to our smoothing (20-30km) and the quite small inversion grid (4x4x2 km), there
 10 are no major consequences for our interpretation.

11 Inversion algorithm:

12 5 Results

13 *Initial Earthquake location*

14 The initial earthquake location is realised and tested with two different velocity models : 1D
 15 VELEST and 3D a-priori. The plate earth approximation is only tested with the Minimum
 16 1D model and all models are tested with and without station corrections. Results are all
 17 compared to the 1D HYPO71 routine of the OMP. This last is the result of few runs of
 18 HYPO71 with different initial depth between 0 and 20 km at each 1km. The final result is
 19 the barycenter of the 21 solutions. The station corrections estimation for the 3D a-priori
 20 velocity models is based on an average of all residues using the result for which the procedure
 21 previously described using both P and S phases within 120 km from the epicenter has been
 22 applied.

23 Initial earthquake location are tested thanks to reference events previously defined. Each
 24 test is applied on three datasets:

- 25 1. three quarry blasts
- 26 2. entire catalog including the three reference sequences of events and
- 27 3. a dataset based on a selection of few events among the three reference sequences of
 28 events. For this third dataset, we select all events, among Argelès, Cauterets and Agly
 29 seismic sequences, having at least 10 stations with PG and SG phases for which the
 30 hypocenter is well constrained (this last is called “optimal solution” after). From this
 31 selection, we build a dataset with all possible seismic stations combination between
 32 3 and 10 using the 10 closest seismic stations. For consequence, one event selected
 33 with its 10 closest seismic stations with its PG and SG gives 968 “sub-events” (= $C_10^3 + C_10^4 + C_10^5 + C_10^6 + C_10^7 + C_10^8 + C_10^9 + 1$). Statistics on azimuthal gap,
 34 number of stations used and distance to the first station will be compared with the
 35

1 absolute distance to the optimal solution, the epicentral distance difference and the
2 depth difference.

3 The figure 7 shows results of the absolute earthquake location of three quarry blasts.
4 For the two quarry blasts of Luzenac, using station corrections greatly improve the absolute
5 earthquake location. That is not the case for the quarry blast of Bustince. We remark that
6 using ellipsoidal earth approximation improves the depth determination in all cases. At last,
7 we note that the 3D tomo model deduced from the inversion of all phases (Figure 17) damages
8 the absolute earthquake location. The hypocenter is still close to the absolute earthquake
9 location estimated within the 3D a-priori velocity model without station corrections. Few
10 hypothesis can explain such result. Among them, we could first consider that the use of
11 refracted phases has degraded the upper-crust velocity structure first deduced using only
12 crustal phases. The figure 8 shows other complementary results in order to understand what
13 exactly happened. Clearly, absolute earthquake location within the 3D a-priori model based
14 on the NonLinLoc procedure previously defined are quite bad. Quarry blast is mislocated
15 with about 2km horizontally and 3 km too shallow. In consequence, stations corrections are
16 also bad-estimated and these last do not improve the earthquake location. The fact to not
17 use S phases additionally to no station corrections improves the absolute earthquake location
18 within the a-priori velocity model with an accuracy about 1km horizontally and 2.7 km too
19 deep.

20
21 Figures 9 to 12 give the visual comparisons on map and on vertical cross-sections for the
22 three seismic sequences used as reference. Clearly, the absolute earthquake location using
23 the 1D VELEST minimum velocity model seems to be the best one. In the Agly sequence,
24 clustering in depth is well retrieved and a WNW-ESE trending alignment appears parallel
25 to one of the nodal plane of the main shock (i.e. [2007]). In argelès-Gazost sequence, the
26 clustering in depth is quite nice and quite similar to the 3D result of [2008]. At last, for the
27 Cauterets sequence, the horizontal clustering is very good contrarily to the deep clustering
28 that is not well retrieved according to the relative re-location of [2004].

29
30 Figure 12 shows results of the third test based on synthetic dataset. Again, calculations
31 are realised within the 3D tomo model which is drawn in figure 17. We can note that the
32 horizontal and vertical estimation of the hypocenter is only slightly preserved within the 3D
33 tomo model according to other earthquake location.

34 At this time, we do not use yet results of 1D VELEST model with ellipsoid earth ap-
35 proximation for the initial earthquake location in the tomography while it seems to be the
36 most accurate . Following 3D velocity models results are based on the 1D minimum velocity
37 model.

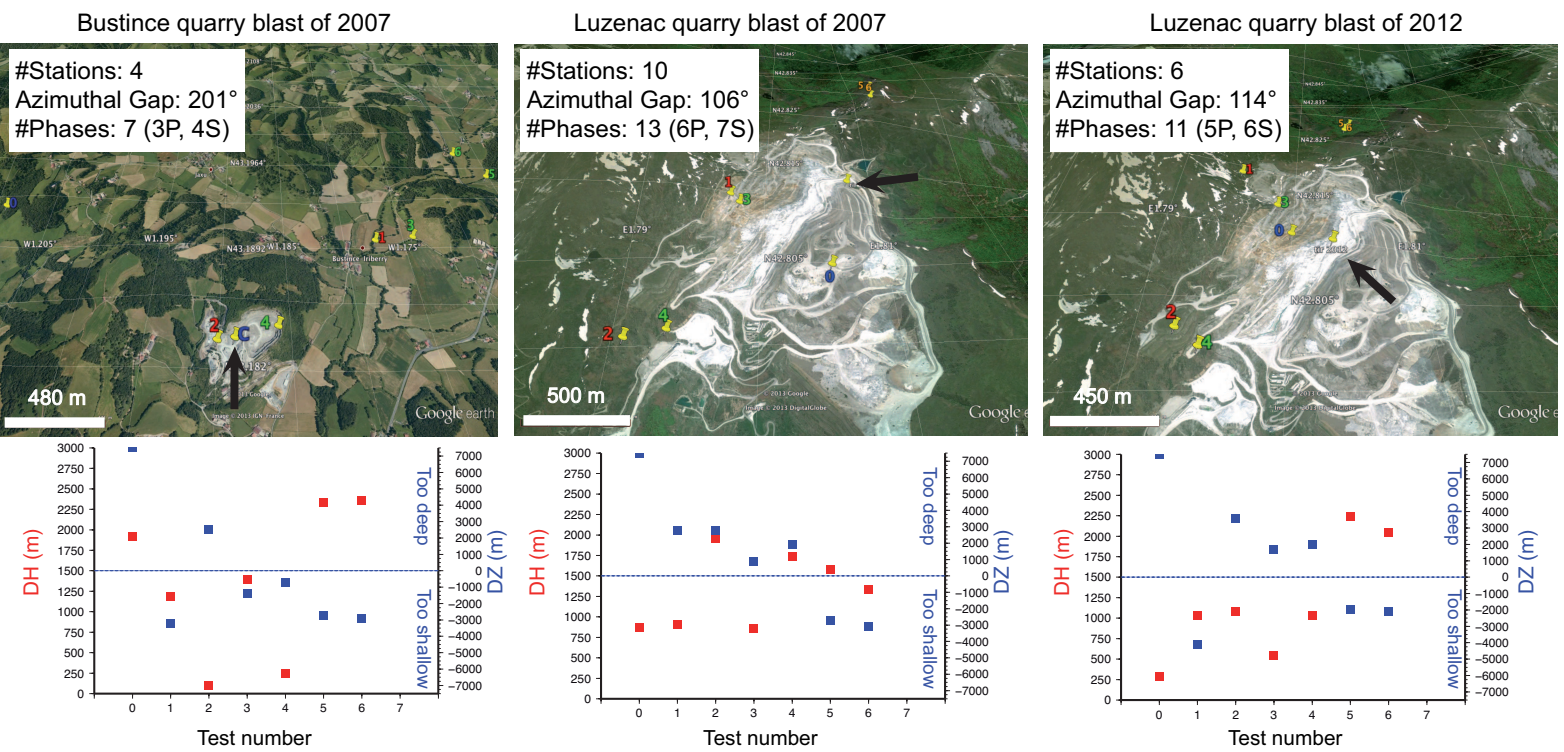


Figure 7: Results of absolute quarry blasts location. 0: OMP; 1: 1D Velost (plate earth) + delays; 2: 1D Velost (plate earth) no delays; 3: 1D Velost (ellipsoidal earth)+delays; 4: 1D Velost (ellipsoidal earth) no delays; 5: 3D tomographic model; 6: 3D a-priori no delays. The 3D model n^5 comes from the inversion of velocities for the entire crust using both P_G/S_G and P_n/S_n phases using the 3D a-priori model as initial velocity model. DH: horizontal misfit. DZ: vertical misfit.

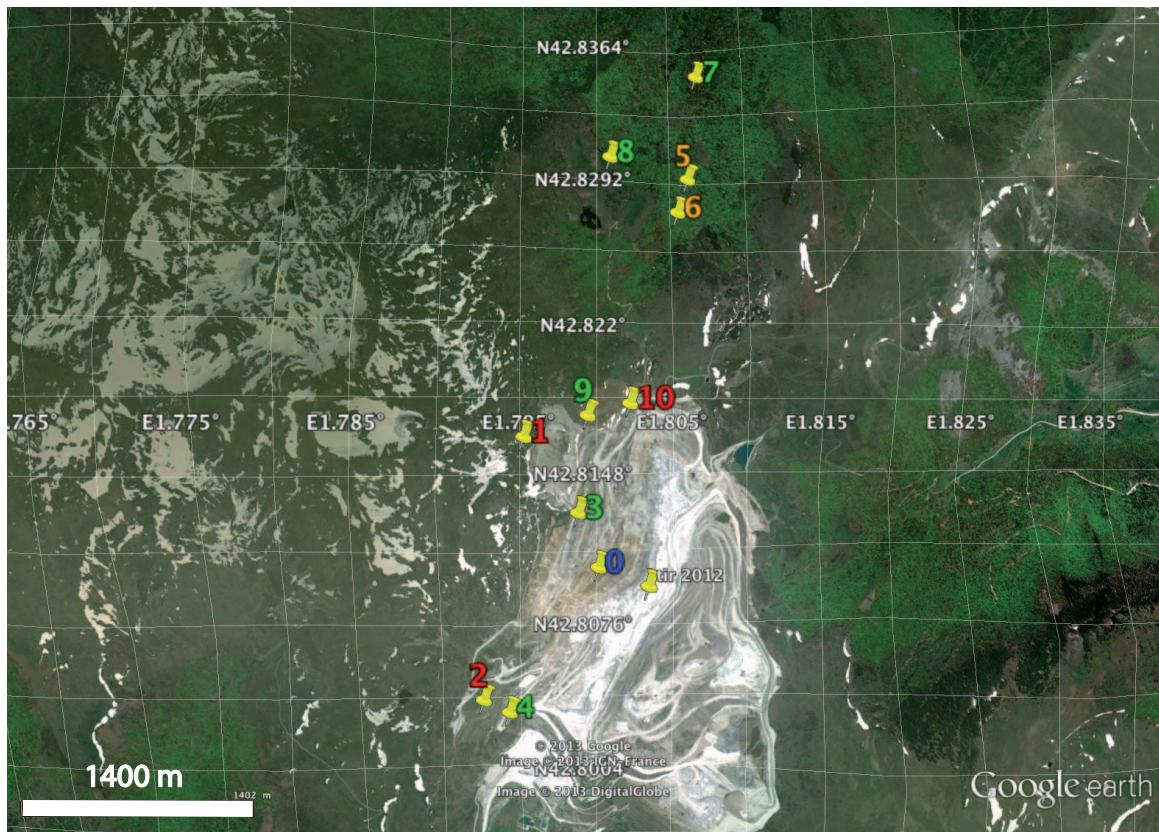


Figure 8: Other results based on absolute location of the Luzenac quarry blast of 2012. 0: OMP (**9km depth**); 1: 1D Velest (plate earth) + delays (**6km altitude**); 2: 1D Velest (plate earth) no delays (**1.9km depth**); 3: 1D Velest (ellipsoidal earth)+delays(**100 m altitude**); 4: 1D Velest (ellipsoidal earth) no delays (**180 m depth**); 5: 3D tomographic model (**4.8km altitude**); 6: 3D a-priori no delays (**4.9km altitude**) ; 7: 3D a-priori + delays (**4.7km altitude**) ; 8: 3D a-priori + delays no S (**0.9km altitude**) ; 9: 3D a-priori no delays no S (**0.9km depth**) ; 10: 3D tomographic model no S (**4.6km depth**). The 3D models n°5 and n°10 come from the inversion of velocities for the entire crust using both P_G/S_G and P_n/S_n phases.

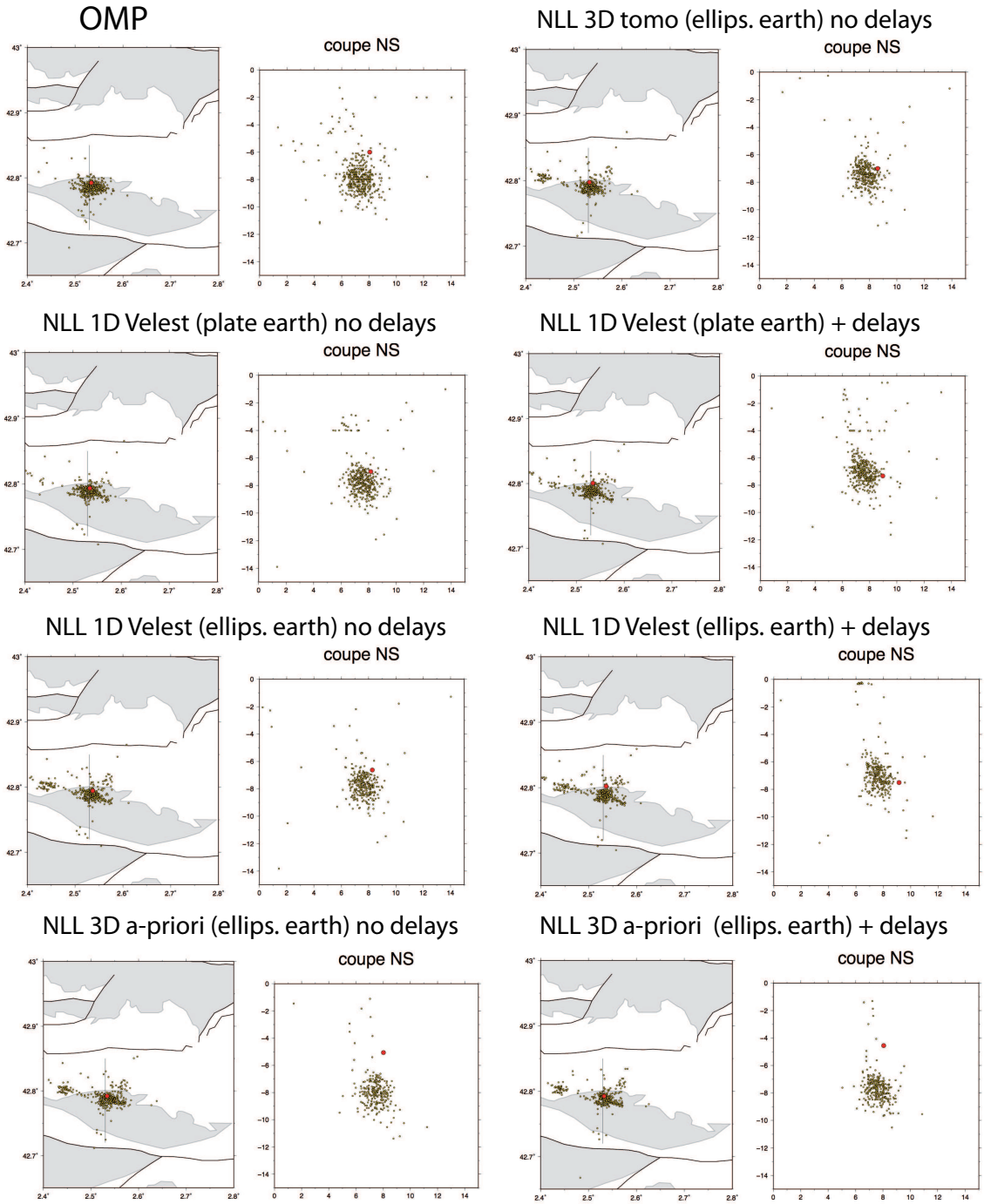


Figure 9: Results for the Agly sequence. The 3D tomo model comes from the inversion of velocities for the entire crust using both P_G/S_G and P_n/S_n phases using the 3D a-priori model as initial velocity model.

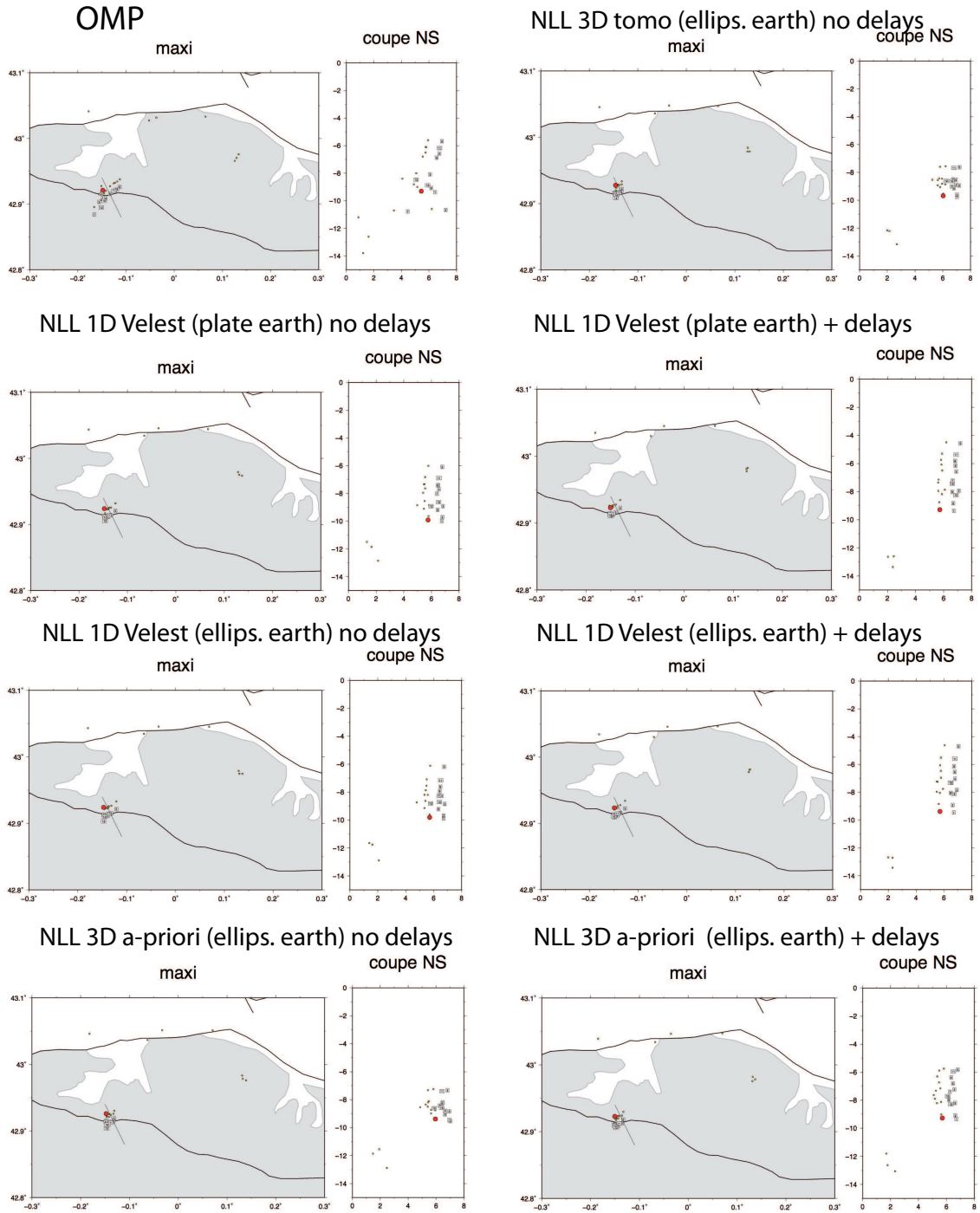


Figure 11: Results for the Cauterets sequence. The 3D tomo model comes from the inversion of velocities for the entire crust using both P_G/S_G and P_n/S_n phases using the 3D a-priori model as initial velocity model.

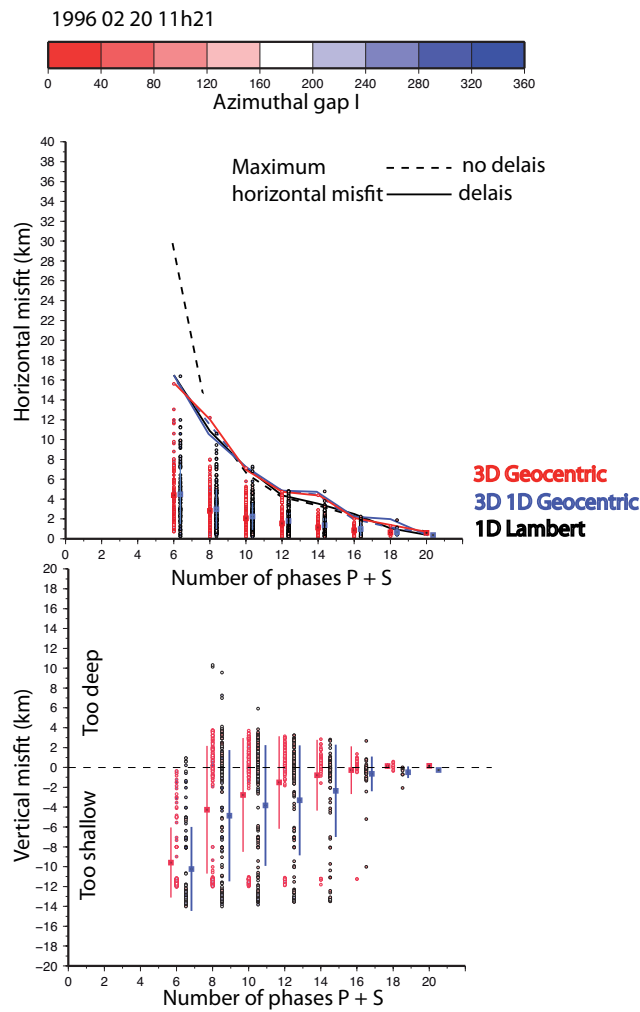


Figure 12: Results of the synthetic absolute earthquake locations for the well located 20th February 1996 earthquake from the Agly sequence within the 3D tomo model (called 3D geocentric). This last comes from the inversion of velocities for the entire crust using both P_G/S_G and P_n/S_n phases using the 3D a-priori model as initial velocity model. The model called 3D 1D geocentric is the 1D VELEST model with ellipsoidal earth approximation.

Upper-crust model

Upper-crust models presented in figures ?? are calculated by fixing the initial hypocenter location and using only P_G and S_G phases with an epicentral distance lower than 121 km. The earthquake position has been kept fixed while the origin time is free to change during the process. 35 iterations have been calculated for both inversions. The variance reduction is better (66% versus 59%) when starting with the 1D VELEST minimum velocity model but the final rms (0.238 s versus 0.251 s) is slightly better with the 3D a-priori model. Two important features appear both inversions: first few positive V_P anomalies are well visible along the North Pyrenean zone within the basement (V_P around 6.2-6.3 km/s versus 6.0 km/s around) and second, VP velocities are quite low (about 6.0 km/s) within the pyrenees (see at 10 km depth in figures 13 and 14) in comparison with initial velocity (between 6.09 km/s in the 1D VELEST model and 6.17 km/s in the 3D a-priori model). Positives V_P anomalies are associated with high V_P/V_S ratio around 1.78 while basement seems characterized by a V_P/V_S ratio of 1.69-1.70. Such values well describes basic rocks as graulites or peridotites. Major two anomalies are located below area with positive Bouguer anomalies in link with a higher density.

Earthquakes location has not been test yet within these two models.

Crust model

Entire crust models presented in figures ?? are calculated by fixing the initial hypocenter location and using all P_N/S_N and P_G/S_G phases. The initial velocity model is based on the previous result of the upper-crust. The origin time and the earthquake position are fixed during the process. At the first order, the use of 2D smooth a-priori Moho seems to improve results of the inversion. Thank to the comparison between figures 15, 16 and 17, we can see that the crustal root, west of the Pyrenees, is partially recovered using our dataset when using a Moho at 35 km (figure 15). We note that the addition of refracted phase disturbs the upper-crust previously estimated with only crustal and close phases both in amplitude and sometimes by changing sign of anomalies. However, it is important to remark that the cut-off distance at an epicentral disatnce of 120 km removes also some deep E-W crustal P_G/S_G phases. Disturbances within upper-crust could also be associated with theses phases. The variance reduction is quite low, about 45% when using the 2D smooth a-priori moho, for distant phases (>120 km) in this inversionte . As for th eupper-crust inversion, the 3D a-priori

Absolute earthquake location has been only tested in the 3D model shown in figure17.

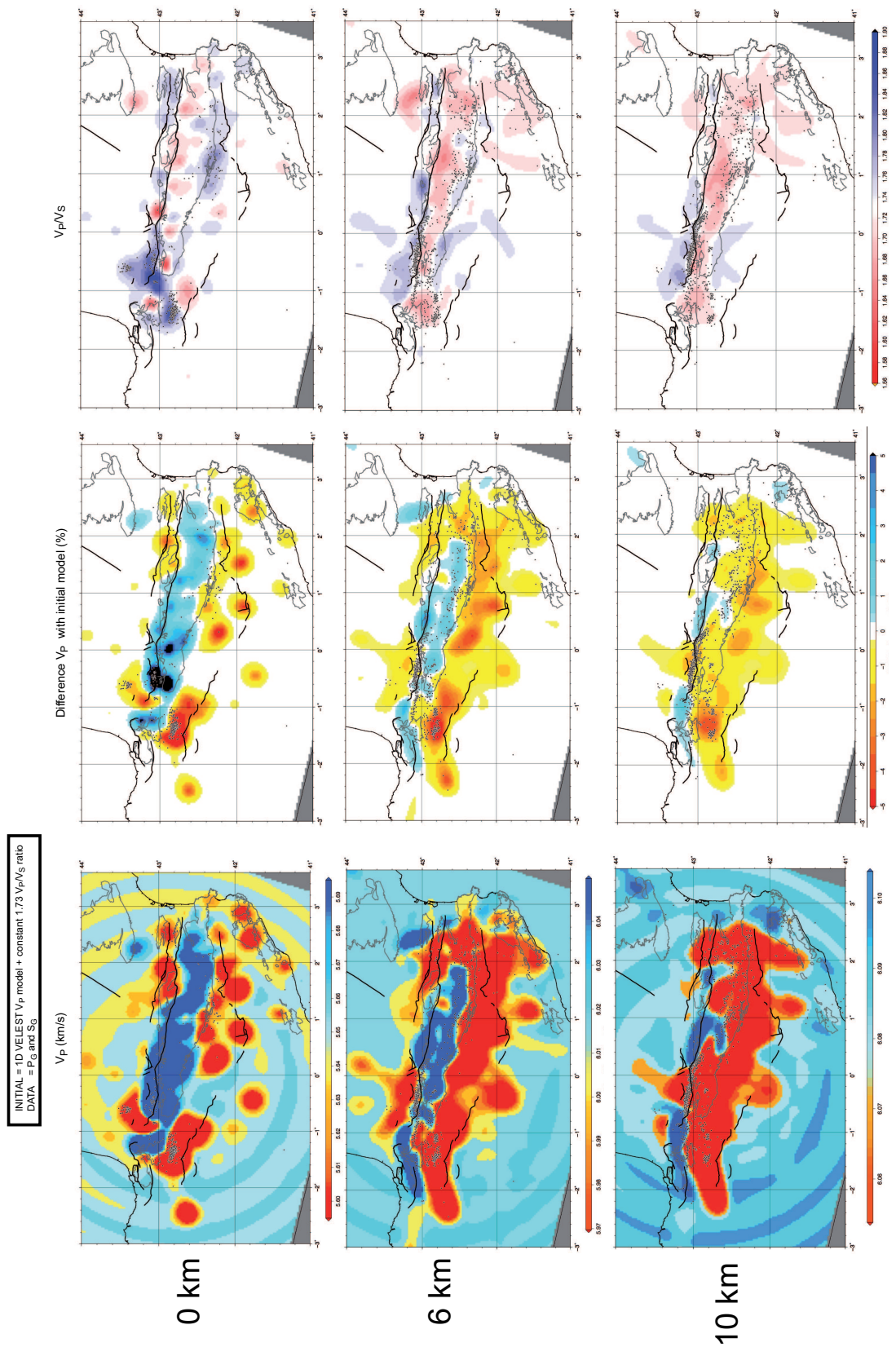


Figure 13: Horizontal slices at 0, 6 and 10 km depth within the upper-crust velocity model obtained using P_G/S_G inversion from 1D VELEST P velocity model and a constant V_P/V_S ratio of 1.73 for the entire crust. The variance reduction is 66% and the final rms is 0.251 s.

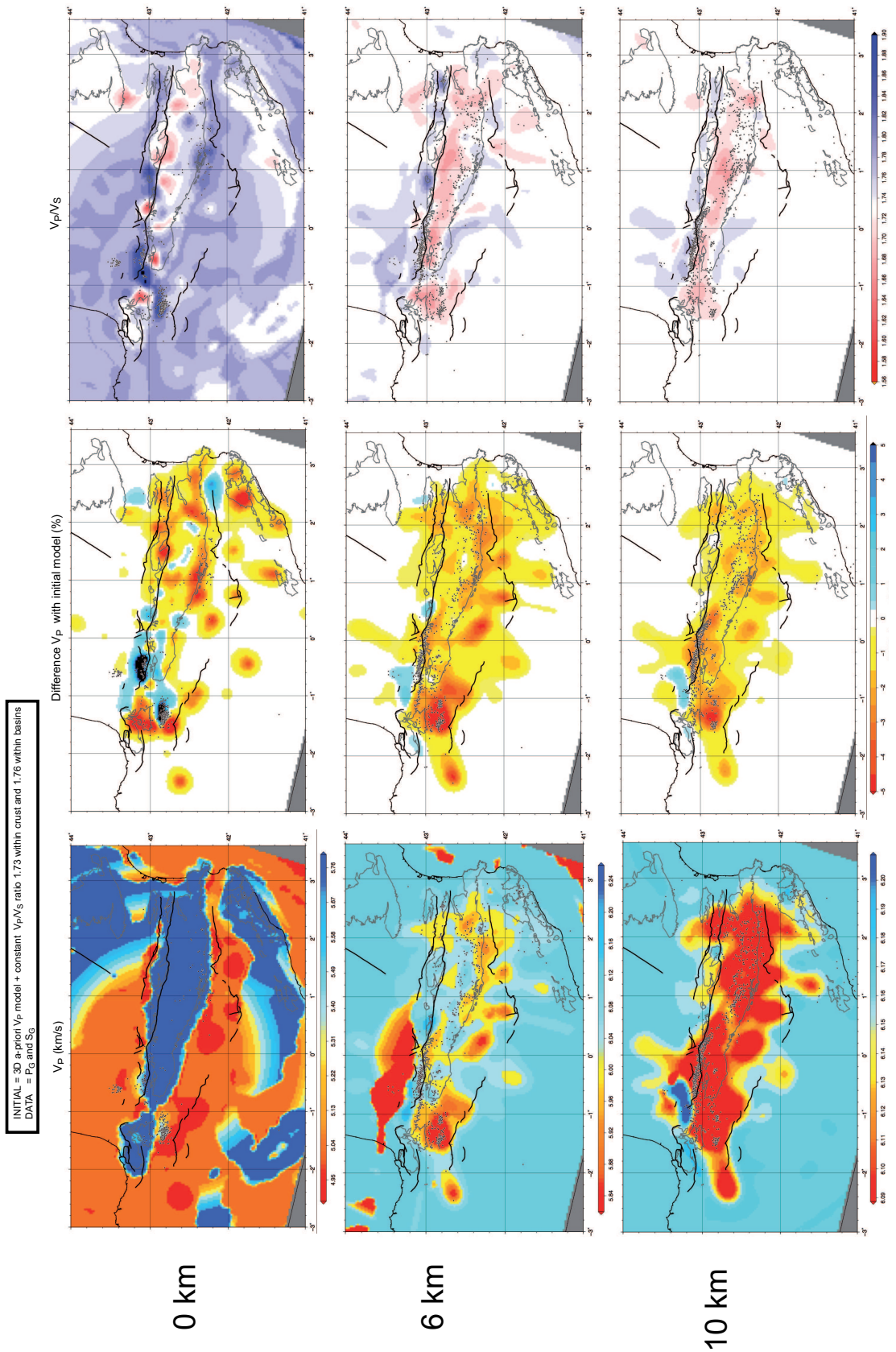


Figure 14: Horizontal slices at 0, 6 and 10 km depth within the upper-crust velocity model obtained using P_G/S_G inversion from 3D a-priori model and a constant V_P/V_S ratio of 1.73 for the crust and 1.76 for sedimentary basins. The variance reduction is 59% and final rms is 0.238 s.

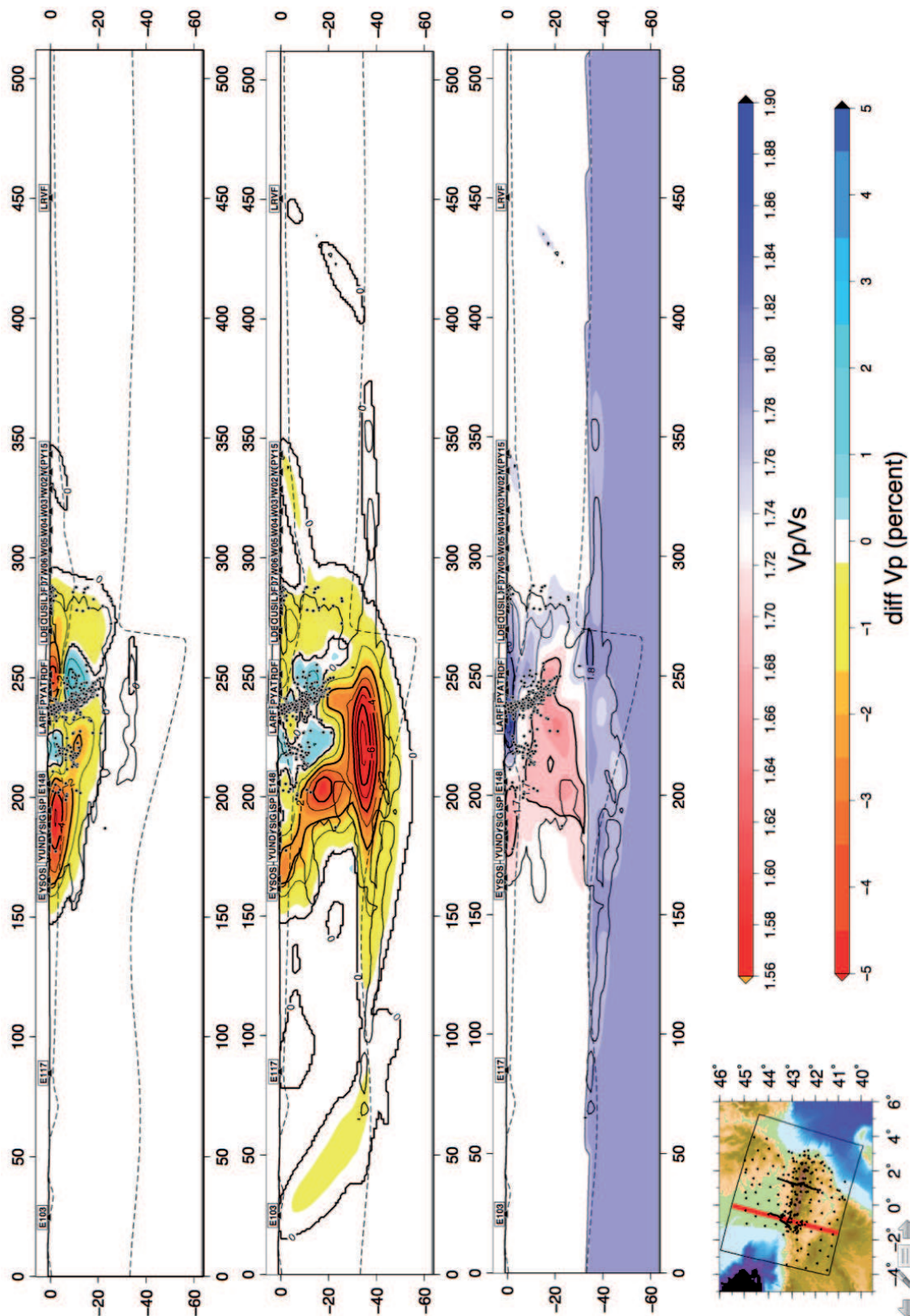


Figure 15: Vertical cross-section west of the Pyrenees through the Mauleon basin within the crust model obtained using all phases during inversion from 1D VELEST P-model and a constant V_P/V_S ratio of 1.73 for the crust and a moho at 35 km depth. Up : the initial velocity P-waves model (same as in figure 13). The variance reduction is about 67% and the final rms 0.400 s.

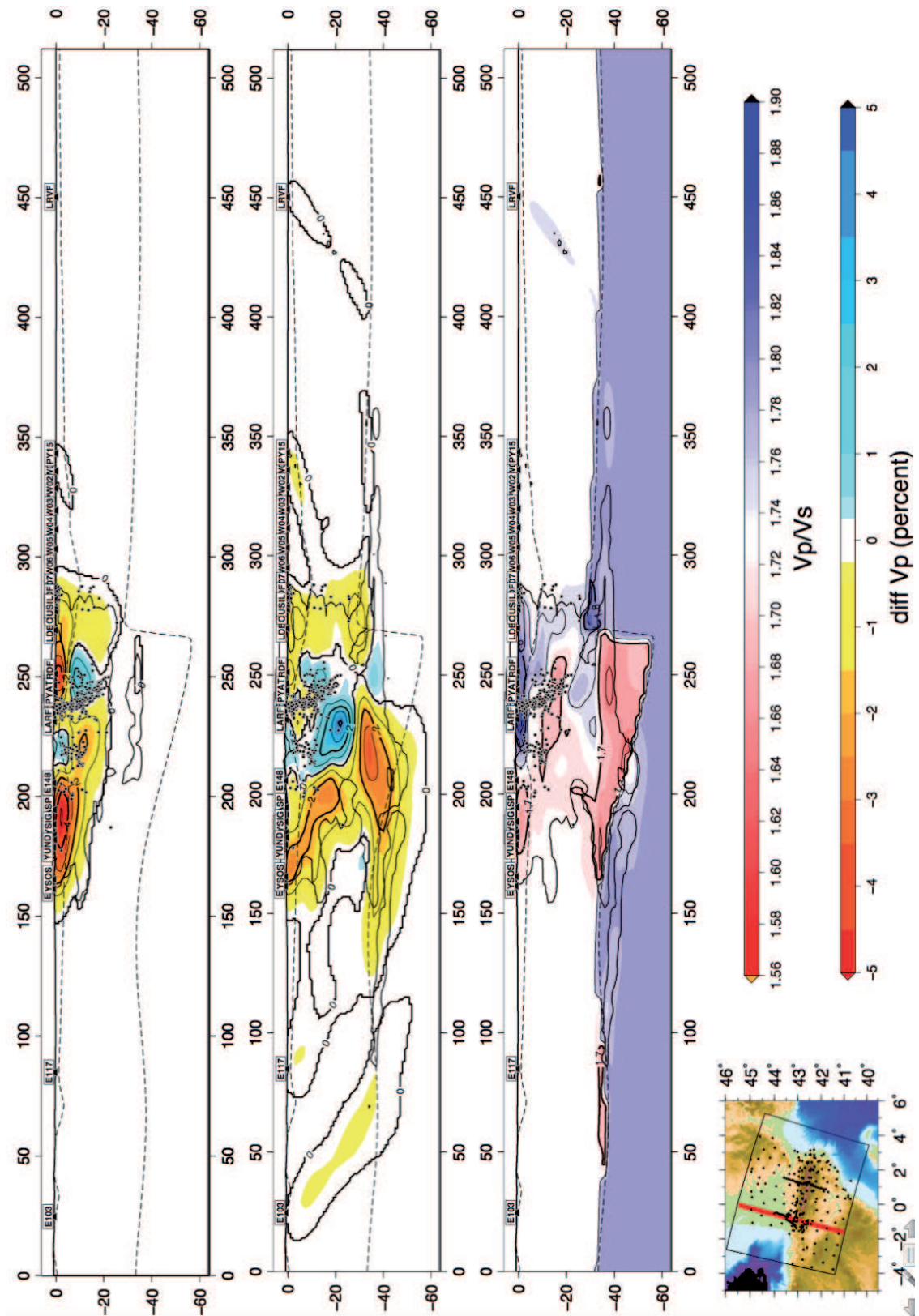


Figure 16: Vertical cross-section west of the Pyrenees through the Mauleon basin within the crust model obtained using all phases during inversion from 1D VELEST P-model and a constant V_P/V_S ratio of 1.73 for the crust and a 2D smooth moho similar to the 3D a-priori model. Up : the initial velocity P-waves model (same as in figure 13). The variance reduction is about 45% and the final rms 0.399 s.

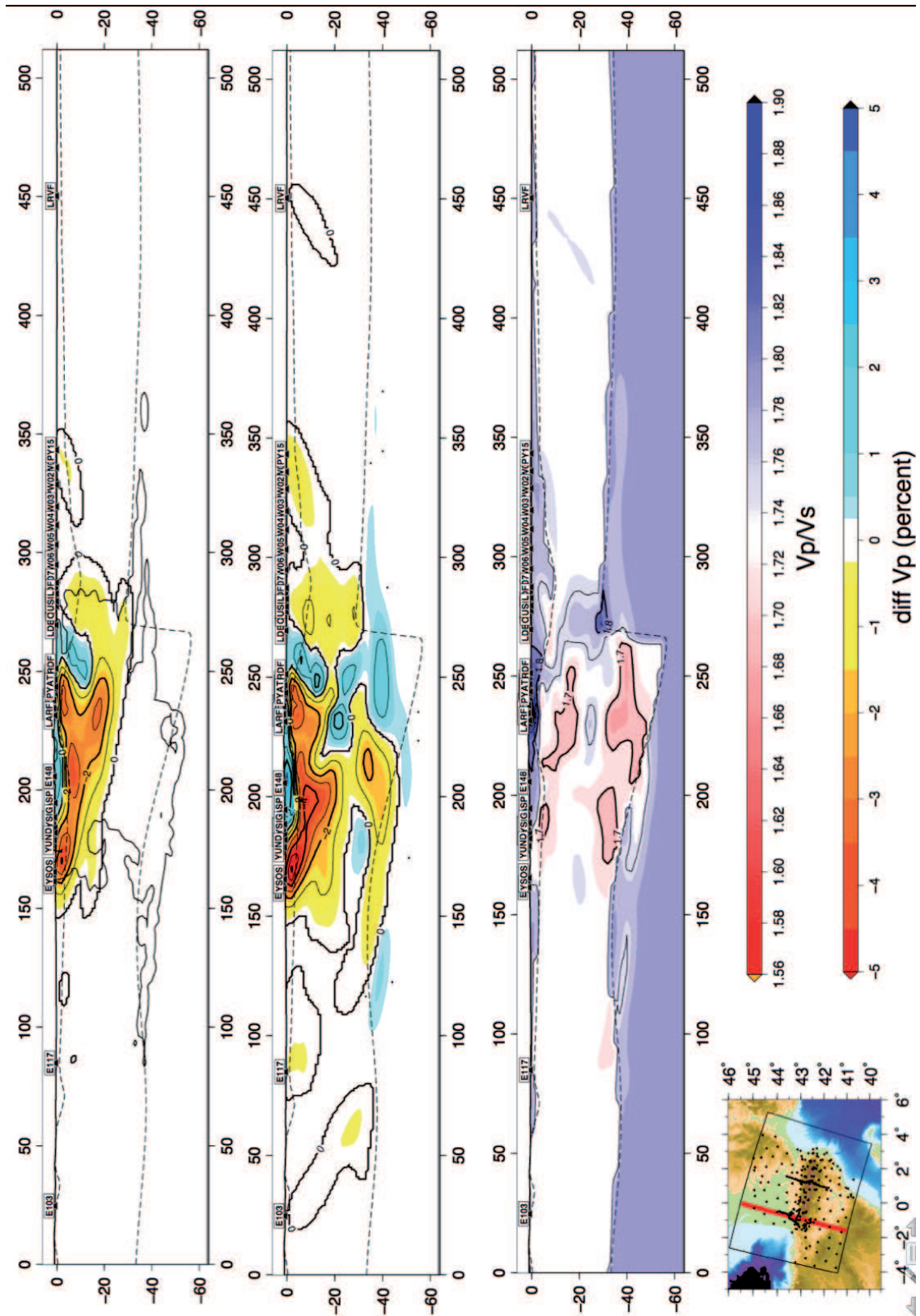


Figure 17: Vertical cross-section west of the Pyrenees through the Mauleon basin within the crust model obtained using all phases during inversion from 3D a-priori model and a constant V_P/V_S ratio of 1.73 for the crust and 1.76 for sedimentary basins and the 2D smooth mocho discontinuity. Up : the initial velocity P-waves model (same as in figure 14). The variance reduction is about 45% and the final rms 0.389 s.

6 Discussion and prospects for this work

This work is still in progress.

Absolute Earthquake location

1. The absolute earthquake location within the 3D a-priori model has to be updated. The S-velocity model should be not use in the process. Station corrections should be calculated using only a selection of best located earthquakes (as for the 1D inversion using VELEST).
2. absolute earthquake location tests should be realised within the upper-crust model
3. the earthquake position should be free during inversion of the upper-crust after few iterations and analysed
4. absolute earthquake mislocation from NonLinLoc should be also described using gaussian uncertainties provided by the process

Determination of the 3D velocity model

1. Some data could be added to the dataset, in particular in the west side of the Pyrenees : data from the second PYROPE 2D profile and data from [2006].
2. starting P and S velocity models could be modified taking into account first results shown here (average at each depth within basins and within the basement for example). Indeed, it has been shown that when a large number of high-quality data are used, tomographic inversion results appear to be robust with respect to the initial reference model [Lees and Shalev, 1992]. In our case, our dataset is maybe insufficient to correctly retrieve a robust 3D model according to the initial velocity model in particular in depth.
3. Variance reduction using refracted phases on the Moho is quite low (45%) when using 2D a-priori smooth moho and a-priori upper-crust model because the final rms about 0.4 s seems to be still too high. This result has to be understand as well as possible in order to improve the inversion (to modify input dataset?, to use another kind of inversion?)
4. The velocity model could be test using available refraction data especially in the west Pyrenees [Pedreira et al., 2003].

1 References

- 2 Aki, K. and Lee, W. (1976). DETERMINATION OF 3-DIMENSIONAL VELOCITY
3 ANOMALIES UNDER A SEISMIC ARRAY USING 1ST-P ARRIVAL TIMES FROM
4 LOCAL EARTHQUAKES .1. A HOMOGENEOUS INITIAL MODEL. *JOURNAL OF*
5 *GEOPHYSICAL RESEARCH*, 81(23):4381–4399.
- 6 Aki, K. and Richards, P. G. (1980). Quantitative seismology; theory and methods. *University*
7 *Science Books*, I and II(-):331–349.
- 8 Amante, C. and Eakins, B. W. (2009). Etopo1 1 arc-minute global relief model: Procedures,
9 data sources and analysis. Technical Report 24, NOAA.
- 10 Asensio, E., Khazaradze, G., Echeverria, A., King, R. W., and Vilajosana, I. (2012). GPS
11 studies of active deformation in the Pyrenees. *GEOPHYSICAL JOURNAL INTERNA-*
12 *TIONAL*, 190(2):913–921.
- 13 Benz, H., Chouet, B., Dawson, P., Lahr, J., Page, R., and Hole, J. (1996). Three-dimensional
14 P and S wave velocity structure of Redoubt Volcano, Alaska. *JOURNAL OF GEOPHYS-*
15 *ICAL RESEARCH-SOLID EARTH*, 101(B4):8111–8128.
- 16 Bodinier, J., Dupuy, C., and Dostal, J. (1988). GEOCHEMISTRY AND PETROGENESIS
17 OF EASTERN PYRENEAN PERIDOTITES. *GEOCHIMICA ET COSMOCHIMICA*
18 *ACTA*, 52(12):2893–2907.
- 19 Bomford, G. (1980). *Geodesy*, volume 4th edition . Clarendon Press (Oxford and New York)
20 .
- 21 Bondar, I. and McLaughlin, K. (2009). Seismic Location Bias and Uncertainty in the Pres-
22 ence of Correlated and Non-Gaussian Travel-Time Errors. *BULLETIN OF THE SEIS-*
23 *MOLOGICAL SOCIETY OF AMERICA*, 99(1):172–193.
- 24 Bondar, I., Myers, S., Engdahl, E., and Bergman, E. (2004). Epicentre accuracy based on
25 seismic network criteria. *GEOPHYSICAL JOURNAL INTERNATIONAL*, 156(3):483–
26 496.
- 27 Bronner, A., Sauter, D., Manatschal, G., Peron-Pinvidic, G., and Munsch, M. (2011). Mag-
28 matic breakup as an explanation for magnetic anomalies at magma-poor rifted margins.
29 *NATURE GEOSCIENCE*, 4(8):549–553.
- 30 Bronner, A., Sauter, D., Manatschal, G., Peron-Pinvidic, G., and Munsch, M. (2012).
31 Problematic plate reconstruction reply. *NATURE GEOSCIENCE*, 5(10):677.

- 1 Campanya, J., Ledo, J., Queralt, P., Marcuello, A., Liesa, M., and Munoz, J. A. (2012). New
2 geoelectrical characterisation of a continental collision zone in the West-Central Pyrenees:
3 Constraints from long period and broadband magnetotellurics. *EARTH AND PLANE-*
4 *TARY SCIENCE LETTERS*, 333:112–121.
- 5 Cara, M., Alasset, P. J., and Sira, C. (2008). Magnitude of Historical Earthquakes, from
6 Macroseismic Data to Seismic Waveform Modelling: Application to the Pyrenees and a
7 1905 Earthquake in the Alps. In Frechet, J and Meghraoui, M and Stucchi, M, editor,
8 *HISTORICAL SEISMOLOGY: INTERDISCIPLINARY STUDIES OF PAST AND RE-*
9 *CENT EARTHQUAKES*, volume 2 of *Modern Approaches in Solid Earth Sciences*, pages
10 369–384, PO BOX 17, 3300 AA DORDRECHT, NETHERLANDS. SPRINGER. Collo-
11 quium on Historical Seismology - From the Archive to the Waveform, Inst Globe Phys,
12 Strasbourg, FRANCE, SEP, 2005.
- 13 Chang, A. C., Shumway, R. H., Blandford, R. R., and Barker, B. W. (1983). Two methods
14 to improve location estimates—preliminary results. *BULLETIN OF THE SEISMOLOG-*
15 *ICAL SOCIETY OF AMERICA*, 73:281–295.
- 16 Chevrot, S., Sylvander, M., and Delouis, B. (2011). A preliminary catalog of moment tensors
17 for the Pyrenees. *TECTONOPHYSICS*, 510(1-2):239–251.
- 18 Choukroune, P. (1990). THE ECORS PROGRAM IN THE PYRENEES - INTRODUC-
19 TION. *BULLETIN DE LA SOCIETE GEOLOGIQUE DE FRANCE*, 6(2):209.
- 20 Clerc, C., Lagabrielle, Y., Neumaier, M., Reynaud, J.-Y., and de Saint Blanquat, M. (2012).
21 Exhumation of subcontinental mantle rocks: evidence from ultramafic-bearing clastic de-
22 posits nearby the Lherz peridotite body, French Pyrenees. *BULLETIN DE LA SOCIETE*
23 *GEOLOGIQUE DE FRANCE*, 183(5):443–459.
- 24 Crosson, R. (1976). CRUSTAL STRUCTURE MODELING OF EARTHQUAKE DATA
25 .1. SIMULTANEOUS LEAST-SQUARES ESTIMATION OF HYPOCENTER AND VE-
26 LOCITY PARAMETERS. *JOURNAL OF GEOPHYSICAL RESEARCH*, 81(17):3036–
27 3046.
- 28 Daignieres, M., Decabissole, B., Gallart, J., Hirn, A., Surinach, E., and Torne, M. (1989).
29 GEOPHYSICAL CONSTRAINTS ON THE DEEP-STRUCTURE ALONG THE ECORS
30 PYRENEES LINE. *TECTONICS*, 8(5):1051–1058.
- 31 Delouis, B., Haessler, H., Cisternas, A., and Rivera, L. (1993). STRESS TENSOR DE-
32 TERMINATION IN FRANCE AND NEIGHBORING REGIONS. *TECTONOPHYSICS*,
33 221(3-4):413–438.

- 1 Diaz, J. and Gallart, J. (2009). Crustal structure beneath the Iberian Peninsula and sur-
2 rounding waters: A new compilation of deep seismic sounding results. *PHYSICS OF THE*
3 *EARTH AND PLANETARY INTERIORS*, 173(1-2):181–190.
- 4 Diaz, J., Pedreira, D., Ruiz, M., Pulgar, J. A., and Gallart, J. (2012). Mapping the inden-
5 tation between the Iberian and Eurasian plates beneath the Western Pyrenees/Eastern
6 Cantabrian Mountains from receiver function analysis. *TECTONOPHYSICS*, 570:114–
7 122.
- 8 Dubos, N., Sylvander, M., Souriau, A., Ponsolles, C., Chevrot, S., Fels, J., and Benahmed,
9 E. (2004). Analysis of the 2002 May earthquake sequence in the central Pyrenees, con-
10 sequences for the evaluation of the seismic risk at Lourdes, France. *GEOPHYSICAL*
11 *JOURNAL INTERNATIONAL*, 156(3):527–540.
- 12 Eberhart-Phillips, D. and Michael, A. J. (1993). Three-dimensional velocity structure, seis-
13 micity, and fault structure in the Parkfield region, central California. *JOURNAL OF*
14 *GEOPHYSICAL RESEARCH*, 98(15):737–758.
- 15 Featherstone, W. E. and Claessens, S. J. (2008). Closed-form transformation between geode-
16 tic and ellipsoidal coordinates. *STUDIA GEOPHYSICA ET GEODAETICA*, 52(1):1–18.
- 17 Fitzgerald, P., Munoz, J., Coney, P., and Baldwin, S. (1999). Asymmetric exhumation
18 across the Pyrenean orogen: implications for the tectonic evolution of a collisional orogen.
19 *EARTH AND PLANETARY SCIENCE LETTERS*, 173(3):157–170.
- 20 Flanagan, M. P., Myers, S. C., and Koper, K. D. (2007). Regional travel-time uncertainty
21 and seismic location improvement using a three-dimensional a priori velocity model. *BUL-*
22 *LETIN OF THE SEISMOLOGICAL SOCIETY OF AMERICA*, 97(3):804–825.
- 23 Font, Y., Kao, H., Lallemand, S., Liu, C., and Chiao, L. (2004). Hypocentre determination
24 offshore of eastern Taiwan using the Maximum Intersection method. *GEOPHYSICAL*
25 *JOURNAL INTERNATIONAL*, 158(2):655–675.
- 26 Font, Y., Segovia, M., Vaca, S., and Theunissen, T. (2013). Seismicity patterns along the
27 Ecuadorian subduction zone: new constraints from earthquake location in a 3-D a priori
28 velocity model. *GEOPHYSICAL JOURNAL INTERNATIONAL*, 193(1):263–286.
- 29 Frohlich, C. (1979). EFFICIENT METHOD FOR JOINT HYPOCENTER DETERMINA-
30 TION FOR LARGE GROUPS OF EARTHQUAKES. *COMPUTERS & GEOSCIENCES*,
31 5(3-4):387–389.
- 32 Gallart, J., Banda, E., and Daignieres, M. (1981). CRUSTAL STRUCTURE OF
33 THE PALEOZOIC-AXIAL-ZONE OF THE PYRENEES AND TRANSITION TO THE
34 NORTH-PYRENEAN-ZONE. *ANNALES DE GEOPHYSIQUE*, 37(3):457–480.

- 1 Gallart, J., Daignieres, M., Banda, E., Surinach, E., and Hirn, A. (1980). THE EASTERN
2 PYRENEAN DOMAIN - LATERAL VARIATIONS AT CRUST-MANTLE LEVEL. *AN-*
3 *NALES DE GEOPHYSIQUE*, 36(2):141–157.
- 4 Gallastegui, J. (2000). Estructura cortical de la cordillera y margen continental cantabricos:
5 Perfiles esci-n. *Trabajos de Geologia*, 22:1–121.
- 6 Gautier, S., Latorre, D., Virieux, J., Deschamps, A., Skarpeles, C., Sotiriou, A., Serpetsidaki,
7 A., and Tselentis, A. (2006). A new passive tomography of the aigion area (Gulf of Corinth,
8 Greece) from the 2002 data set. *PURE AND APPLIED GEOPHYSICS*, 163(2-3):431–
9 453. Annual Meeting of the American-Geophysical-Union, San Francisco, CA, DEC 13-17,
10 2004.
- 11 Geiger, L. (1910). Herdbestimmung bei Erdbeben aus den Ankunftszeiten. *Nachrichten von*
12 *der Koniglichen Gesellschaft der Wissenschaften zu Gottingen*, 4(-):557pp and 373pp.
- 13 Granjean, G. (1994). STUDY OF CRUSTAL STRUCTURES IN A SECTION OF A
14 MOUNTAIN-RANGE - RELATIONSHIP WITH SEDIMENTARY BASINS - APPLICA-
15 TION TO WESTERN PYRENEES. *BULLETIN DES CENTRES DE RECHERCHES*
16 *EXPLORATION-PRODUCTION ELF AQUITAINE*, 18(2):391–419.
- 17 Gunnell, Y. and Calvet, M. (2006). Comment on “Origin of the highly elevated Pyrenean
18 peneplain” by Julien Babault, Jean Van Den Driessche, and Stephane Bonnet, Sebastien
19 Castelltort, and Alain Crave. *TECTONICS*, 25(3).
- 20 Hirn, A., Daignieres, M., Gallart, J., and Vadell, M. (1980). EXPLOSION SEISMIC-
21 SOUNDING OF THROWS AND DIPS IN THE CONTINENTAL MOHO. *GEOPHYSI-*
22 *CAL RESEARCH LETTERS*, 7(4):263–266.
- 23 Huang, Z. and Zhao, D. (2012). Relocating the 2011 Tohoku-oki earthquakes (m 6.0-9.0).
24 *Tectonophysics*, 586:35–45.
- 25 Husen, S., Kissling, E., and Clinton, J. F. (2011). Local and regional minimum 1D models for
26 earthquake location and data quality assessment in complex tectonic regions: application
27 to Switzerland. *SWISS JOURNAL OF GEOSCIENCES*, 104(3):455–469.
- 28 Husen, S., Kissling, E., Deichmann, N., Wiemer, S., Giardini, D., and Baer, M. (2003). Prob-
29 abilistic earthquake location in complex three-dimensional velocity models: Application
30 to Switzerland. *JOURNAL OF GEOPHYSICAL RESEARCH-SOLID EARTH*, 108(B2).
- 31 Husen, S., Kissling, E., Flueh, E., and Asch, G. (1999). Accurate hypocentre determination
32 in the seismogenic zone of the subducting Nazca Plate in northern Chile using a combined
33 on-/offshore network. *GEOPHYSICAL JOURNAL INTERNATIONAL*, 138(3):687–701.

- 1 Jammes, S., Lavier, L., and Manatschal, G. (2010). Extreme crustal thinning in the Bay
2 of Biscay and the Western Pyrenees: From observations to modeling. *GEOCHEMISTRY*
3 *GEOPHYSICS GEOSYSTEMS*, 11.
- 4 Jammes, S., Manatschal, G., Lavier, L., and Masini, E. (2009). Tectonosedimentary evolution
5 related to extreme crustal thinning ahead of a propagating ocean: Example of the western
6 Pyrenees. *TECTONICS*, 28.
- 7 Kissling, E. (1988). GEOTOMOGRAPHY WITH LOCAL EARTHQUAKE DATA. *RE-*
8 *VIEWS OF GEOPHYSICS*, 26(4):659–698.
- 9 Kissling, E., Ellsworth, W., Eberhart-Phillips, D., and Kradolfer, U. (1994). INITIAL
10 REFERENCE MODELS IN LOCAL EARTHQUAKE TOMOGRAPHY. *JOURNAL OF*
11 *GEOPHYSICAL RESEARCH-SOLID EARTH*, 99(B10):19635–19646.
- 12 KISSLING, E., SOLARINO, S., and CATTANEO, M. (1995). IMPROVED SEISMIC VE-
13 LOCITY REFERENCE MODEL FROM LOCAL EARTHQUAKE DATA IN NORTH-
14 WESTERN ITALY. *TERRA NOVA*, 7(5):528–534.
- 15 Lacan, P. and Ortuno, M. (2012). Active Tectonics of the Pyrenees: A review. *JOURNAL*
16 *OF IBERIAN GEOLOGY*, 38(1, SI):9–30.
- 17 Lagabrielle, Y., Labaume, P., and de Saint Blanquat, M. (2010). Mantle exhumation, crustal
18 denudation, and gravity tectonics during Cretaceous rifting in the Pyrenean realm (SW
19 Europe): Insights from the geological setting of the lherzolite bodies. *TECTONICS*, 29.
- 20 Latorre, D., Virieux, J., Monfret, T., Monteiller, V., Vanorio, T., Got, J., and Lyon-Caen,
21 H. (2004). A new seismic tomography of Aigion area (Gulf of Corinth, Greece) from the
22 1991 data set. *GEOPHYSICAL JOURNAL INTERNATIONAL*, 159(3):1013–1031.
- 23 Ledo, J., Ayala, C., Pous, J., Queralt, P., Marcuello, A., and Munoz, J. (2000). New geo-
24 physical constraints on the deep structure of the Pyrenees. *GEOPHYSICAL RESEARCH*
25 *LETTERS*, 27(7):1037–1040.
- 26 Lees, J. M. and Shalev, E. (1992). On the stability of P-wave tomography at Loma-Prieta—a
27 comparison of parameterizations, linear and nonlinear inversions. *BULLETIN OF THE*
28 *SEISMOLOGICAL SOCIETY OF AMERICA*, 82:1821–1839.
- 29 Lin, G., Shearer, P., and Fialko, Y. (2006). Obtaining absolute locations for quarry seismic-
30 ity using remote sensing data. *BULLETIN OF THE SEISMOLOGICAL SOCIETY OF*
31 *AMERICA*, 96(2):722–728.
- 32 Lin, Y.-P., Zhao, L., and Hung, S.-H. (2011). Assessment of Tomography Models of Taiwan
33 Using First-Arrival Times from the TAIGER Active-Source Experiment. *BULLETIN OF*
34 *THE SEISMOLOGICAL SOCIETY OF AMERICA*, 101(2):866–880.

- 1 Lomax, A. (2005). A reanalysis of the hypocentral location and related observations for the
2 great 1906 California earthquake. *BULLETIN OF THE SEISMOLOGICAL SOCIETY*
3 *OF AMERICA*, 95(3):861–877.
- 4 Lomax, A., Virieux, J., Volant, P., and Berge-Thierry, C. (2000). Probabilistic earthquake
5 location in 3D and layered models - Introduction of a Metropolis-Gibbs method and com-
6 parison with linear locations. In Thurber, CH and Rabinowitz, N, editor, *ADVANCES IN*
7 *SEISMIC EVENT LOCATION*, pages 101–134, PO BOX 17, 3300 AA DORDRECHT,
8 NETHERLANDS. Shalheveth Freier Ctr Peace Sci & Technol, SPRINGER. 1st Interna-
9 tional Workshop on Advanced Methods in Seismic Analysis, DEAD SEA, ISRAEL, JAN,
10 1998.
- 11 Monteiller, V. (2005). *Tomograohie à l'aide de décalages temporels d'ondes sismiques P :*
12 *développements méthodologiques et applications*. PhD thesis, Savoie University.
- 13 Monteiller, V., Got, J., Virieux, J., and Okubo, P. (2005). An efficient algorithm for double-
14 difference tomography and location in heterogeneous media, with an application to the Ki-
15 lauea volcano. *JOURNAL OF GEOPHYSICAL RESEARCH-SOLID EARTH*, 110(B12).
- 16 Moser, T., Vaneck, T., and Nolet, G. (1992). HYPOCENTER DETERMINATION IN
17 STRONGLY HETEROGENEOUS EARTH MODELS USING THE SHORTEST-PATH
18 METHOD. *JOURNAL OF GEOPHYSICAL RESEARCH-SOLID EARTH*, 97(B5):6563–
19 6572.
- 20 Mostaccio, A., Tuve, T., Patane, D., Barberi, G., and Zuccarello, L. (2013). Improving
21 Seismic Surveillance at Mt. Etna Volcano by Probabilistic Earthquake Location in a 3D
22 Model. *BULLETIN OF THE SEISMOLOGICAL SOCIETY OF AMERICA*, 103(4):2447–
23 2459.
- 24 Munoz, J. (1992). Evolution of a continental collision belt: Ecors-pyrenees crustal balanced
25 cross-section. *Thrust Tectonics*, -:235–246.
- 26 Myers, S. and Schultz, C. (2000). Improving sparse network seismic location with Bayesian
27 kriging and teleseismically constrained calibration events. *BULLETIN OF THE SEIS-*
28 *MOLOGICAL SOCIETY OF AMERICA*, 90(1):199–211.
- 29 Nicolas, M., Santoire, J., and Delpech, P. (1990). INTRAPLATE SEISMICITY - NEW SEIS-
30 MOTECTONIC DATA IN WESTERN-EUROPE. *TECTONOPHYSICS*, 179(1-2):27–53.
31 SYMP AT THE MEETING OF THE EUROPEAN GEOPHYSICAL SOC : SEISMICITY
32 AND CRUSTAL DEFORMATION, BOLOGNA, ITALY, 1988.
- 33 Nocquet, J. and Calais, E. (2004). Geodetic measurements of crustal deformation in the
34 Western Mediterranean and Europe. *PURE AND APPLIED GEOPHYSICS*, 161(3):661–
35 681.

- 1 Pauchet, H., Rigo, A., Rivera, L., and Souriau, A. (1999). A detailed analysis of the February
2 1996 aftershock sequence in the eastern Pyrenees, France. *GEOPHYSICAL JOURNAL*
3 *INTERNATIONAL*, 137(1):107–127.
- 4 Pedreira, D., Ebbing, J., and Pulgar, J. A. (2010). Lithospheric structure of the western
5 pyrenees-cantabrian mountains based on 3d modelling of gravity anomalies and geoid
6 undulations: preliminary results. *Trabajos de Geología*, 30:121–127.
- 7 Pedreira, D., Pulgar, J., Gallart, J., and Diaz, J. (2003). Seismic evidence of Alpine crustal
8 thickening and wedging from the western Pyrenees to the Cantabrian Mountains (north
9 Iberia). *JOURNAL OF GEOPHYSICAL RESEARCH-SOLID EARTH*, 108(B4).
- 10 Pedreira, D., Pulgar, J. A., Gallart, J., and Torne, M. (2007). Three-dimensional gravity and
11 magnetic modeling of crustal indentation and wedging in the western Pyrenees-Cantabrian
12 Mountains. *JOURNAL OF GEOPHYSICAL RESEARCH-SOLID EARTH*, 112(B12).
- 13 Podvin, P. and Lecomte, I. (1991). FINITE-DIFFERENCE COMPUTATION OF TRAVEL-
14 TIMES IN VERY CONTRASTED VELOCITY MODELS - A MASSIVELY PARALLEL
15 APPROACH AND ITS ASSOCIATED TOOLS. *GEOPHYSICAL JOURNAL INTER-*
16 *NATIONAL*, 105(1):271–284.
- 17 Pous, J., Muñoz, J., Ledo, J., and Liesa, M. (1995). Partial melting of subducted continental
18 lower crust in the pyrenees. *J. Geol. Soc. London*, 152:217–220.
- 19 Pujol, J. (1988). COMMENTS ON THE JOINT DETERMINATION OF HYPOCENTERS
20 AND STATION CORRECTIONS. *BULLETIN OF THE SEISMOLOGICAL SOCIETY*
21 *OF AMERICA*, 78(3):1179–1189.
- 22 Pujol, J. (2000). Joint event location - The JHD technique and applications to data from local
23 seismic networks. In Thurber, CH and Rabinowitz, N, editor, *ADVANCES IN SEISMIC*
24 *EVENT LOCATION*, pages 163–204, PO BOX 17, 3300 AA DORDRECHT, NETHER-
25 LANDS. Shalheveth Freier Ctr Peace Sci & Technol, SPRINGER. 1st International Work-
26 shop on Advanced Methods in Seismic Analysis, DEAD SEA, ISRAEL, JAN, 1998.
- 27 Rigo, A., Pauchet, H., Souriau, A., Gresillaud, A., Nicolas, M., Olivera, C., and Figueras,
28 S. (1997). The February 1996 earthquake sequence in the eastern Pyrenees: first results.
29 *JOURNAL OF SEISMOLOGY*, 1(1):3–14.
- 30 Rigo, A., Souriau, A., Dubos, N., Sylvander, M., and Ponsolles, C. (2005). Analysis of
31 the seismicity in the central part of the Pyrenees (France), and tectonic implications.
32 *JOURNAL OF SEISMOLOGY*, 9(2):211–222.
- 33 Roure, F., Chhoukroune, P., Berastegui, X., Munoz, J., Vil, A., Matheron, P., Bareyt, M.,
34 Seguret, M., Camara, P., and Deramond, J. (1989). ECORS DEEP SEISMIC DATA AND

- 1 BALANCED CROSS-SECTIONS - GEOMETRIC CONSTRAINTS ON THE EVOLU-
2 TION OF THE PYRENEES. *TECTONICS*, 8(1):41–50.
- 3 Ruiz, M., Gallart, J., Diaz, J., Olivera, C., Pedreira, D., Lopez, C., Gonzalez-Cortina, J., and
4 Pulgar, J. (2006). Seismic activity at the western Pyrenean edge. *TECTONOPHYSICS*,
5 412(3-4):217–235.
- 6 Satriano, C., Zollo, A., Capuano, P., Russo, G., Vanorio, T., Caielli, G., Lovisa, L., and
7 Moretti, M. (2006). *A 3D velocity model for earthquake location in Campi Flegrei area:*
8 *application to the 1982-84 uplift event*, pages pp 38–49. doppiavoce edition.
- 9 Senechal, G. and Thouvenot, F. (1994). SEISMIC DIFFRACTION FROM THE NORTH
10 PYRENEAN FAULT - A DEPTH-MIGRATED LINE-DRAWING OF THE ECORS
11 PROFILE. *TECTONOPHYSICS*, 233(1-2):83–89.
- 12 Sibuet, J., Srivastava, S., and Spakman, W. (2004). Pyrenean orogeny and plate kinematics.
13 *JOURNAL OF GEOPHYSICAL RESEARCH-SOLID EARTH*, 109(B8).
- 14 Simmons, N. A., Myers, S. C., Johannesson, G., and Matzel, E. (2012). LLNL-G3Dv3:
15 Global P wave tomography model for improved regional and teleseismic travel time pre-
16 diction. *JOURNAL OF GEOPHYSICAL RESEARCH-SOLID EARTH*, 117.
- 17 Souriau, A., Chevrot, S., and Olivera, C. (2008). A new tomographic image of the Pyrenean
18 lithosphere from teleseismic data. *TECTONOPHYSICS*, 460(1-4):206–214.
- 19 Souriau, A. and Granet, M. (1995). A TOMOGRAPHIC STUDY OF THE LITHOSPHERE
20 BENEATH THE PYRENEES FROM LOCAL AND TELESEISMIC DATA. *JOURNAL*
21 *OF GEOPHYSICAL RESEARCH-SOLID EARTH*, 100(B9):18117–18134.
- 22 Souriau, A. and Pauchet, H. (1998). A new synthesis of Pyrenean seismicity and its tectonic
23 implications. *TECTONOPHYSICS*, 290(3-4):221–244.
- 24 Souriau, A., Sylvander, M., Rigo, A., Fels, J., Douchain, J., and Ponsolles, C. (2001).
25 Pyrenean tectonics: main seismological constraints. *BULLETIN DE LA SOCIETE GE-*
26 *OLOGIQUE DE FRANCE*, 172(1):25–39.
- 27 Spakman, W. and Nolet, G. (1988). *Imaging algorithms, accuracy and resolution in delay*
28 *time tomography*, pages 155–188. Mathematical Geophysics. Vlaar et al. (eds.), Reidel,
29 vlaar et al. (eds.) edition.
- 30 Spencer, C. and Gubbins, D. (1980). TRAVEL-TIME INVERSION FOR SIMULTANEOUS
31 EARTHQUAKE LOCATION AND VELOCITY STRUCTURE DETERMINATION IN
32 LATERALLY VARYING MEDIA. *GEOPHYSICAL JOURNAL OF THE ROYAL AS-*
33 *TRONOMICAL SOCIETY*, 63(1):95–116.

- 1 Sylvander, M., Monod, B., Souriau, A., and Rigo, A. (2007). Analysis of an earthquake
2 swarm (May 2004) in the French eastern Pyrenees: Towards a new tectonic interpretation
3 of the Saint-Paul-de-Fenouillet earthquake (1996). *COMPTES RENDUS GEOSCIENCE*,
4 339(1):75–84.
- 5 Sylvander, M., Souriau, A., Rigo, A., Tocheport, A., Toutain, J.-P., Ponsolles, C., and Be-
6 nahmed, S. (2008). The 2006 November, M(L)=5.0 earthquake near Lourdes (France):
7 new evidence for NS extension across the Pyrenees. *GEOPHYSICAL JOURNAL INTER-*
8 *NATIONAL*, 175(2):649–664.
- 9 Tarantola, A. and Valette, B. (1982). GENERALIZED NON-LINEAR INVERSE PROB-
10 LEMS SOLVED USING THE LEAST-SQUARES CRITERION. *REVIEWS OF GEO-*
11 *PHYSICS*, 20(2):219–232.
- 12 Teixell, A. (1998). Crustal structure and orogenic material budget in the west central Pyre-
13 nees. *TECTONICS*, 17(3):395–406.
- 14 Tesauro, M., Kaban, M. K., and Cloetingh, S. A. P. L. (2008). EuCRUST-07: A new
15 reference model for the European crust. *GEOPHYSICAL RESEARCH LETTERS*, 35(5).
- 16 Theunissen, T., Lallemand, S., Font, Y., Gautier, S., Lee, C.-S., Liang, W.-T., Wu, F., and
17 Berthet, T. (2012). Crustal deformation at the southernmost part of the Ryukyu subduc-
18 tion (East Taiwan) as revealed by new marine seismic experiments. *TECTONOPHYSICS*,
19 578(SI):10–30.
- 20 Thurber, C. (1992). HYPOCENTER VELOCITY STRUCTURE COUPLING IN LOCAL
21 EARTHQUAKE TOMOGRAPHY. *PHYSICS OF THE EARTH AND PLANETARY*
22 *INTERIORS*, 75(1-3):55–62. SYMP ON LATERAL HETEROGENEITY AND EARTH-
23 QUAKE LOCATION, AT THE 20TH GENERAL ASSEMBLY OF THE INTERNA-
24 TIONAL UNION OF GEODESY AND GEOPHYSICS, VIENNA, AUSTRIA, AUG 11-
25 24, 1991.
- 26 Torne, M., Decabissole, B., Bayer, R., Casas, A., Daignieres, M., and Rivero, A. (1989).
27 GRAVITY CONSTRAINTS ON THE DEEP-STRUCTURE OF THE PYRENEAN
28 BELT ALONG THE ECORS PROFILE. *TECTONOPHYSICS*, 165(1-4):105–116.
- 29 Tucholke, B. E. and Sibuet, J.-C. (2012). Problematic plate reconstruction. *NATURE*
30 *GEOSCIENCE*, 5(10):676–677.
- 31 Vacher, P. and Souriau, A. (2001). A three-dimensional model of the Pyrenean deep structure
32 based on gravity modelling, seismic images and petrological constraints. *GEOPHYSICAL*
33 *JOURNAL INTERNATIONAL*, 145(2):460–470.

- 1 Vanorio, T., Virieux, J., Capuano, P., and Russo, G. (2005). Three-dimensional seismic
2 tomography from P wave and S wave microearthquake travel times and rock physics char-
3 acterization of the Campi Flegrei Caldera. *JOURNAL OF GEOPHYSICAL RESEARCH-*
4 *SOLID EARTH*, 110(B3).
- 5 Verges, J., Millan, H., Roca, E., Munoz, J., Marzo, M., Cires, J., Denbezemer, T., Zoete-
6 Meijer, R., and Cloetingh, S. (1995). EASTERN PYRENEES AND RELATED FORE-
7 LAND BASINS - PRECOLLISIONAL, SYNCOLLISIONAL AND POSTCOLLISIONAL
8 CRUSTAL-SCALE CROSS-SECTIONS. *MARINE AND PETROLEUM GEOLOGY*,
9 12(8):903–915.
- 10 Vernant, P., Hivert, F., Chery, J., Steer, P., Cattin, R., and Rigo, A. (2013). Erosion-induced
11 isostatic rebound triggers extension in low convergent mountain ranges. *GEOLOGY*,
12 41(4):467–470.
- 13 Vissers, R. L. M. and Meijer, P. T. (2012). Mesozoic rotation of Iberia: Subduction in the
14 Pyrenees? *EARTH-SCIENCE REVIEWS*, 110(1-4):93–110.
- 15 Wittlinger, G., Herquel, G., and Nakache, T. (1993). EARTHQUAKE LOCATION IN
16 STRONGLY HETEROGENEOUS MEDIA. *GEOPHYSICAL JOURNAL INTERNA-*
17 *TIONAL*, 115(3):759–777.
- 18 Zhou, H. (1994). RAPID 3-DIMENSIONAL HYPOCENTRAL DETERMINATION USING
19 A MASTER STATION METHOD. *JOURNAL OF GEOPHYSICAL RESEARCH-SOLID*
20 *EARTH*, 99(B8):15439–15455.

Review of ‘Comprehensive 3D absolute earthquakes location (versus 1D) and local seismic tomography of the Pyrenean crust from first arrival times’ by T. Theunissen, M. Sylvander and S. Chevrot (SIGMA deliverable D1-89)

The authors compile and analyse a large earthquake catalogue and associated seismic phases from various permanent and temporary seismic networks in the Pyrenees and surrounding area (both in France and Spain). Based on these data they seek to create an improved earthquake catalogue and local tomographic models of the seismic velocities for this region. The report is clearly the fruit of a considerable effort in terms of data compilation and organisation, numerical calculations and interpretation. I particularly appreciated the use of known locations (in this case quarry blasts) to help determine the absolute, rather than just relative, errors. Once this study is completed, the final results clearly have the ability to be of great use for future studies in this region, in terms of tectonics (e.g. fault activity rates), crustal structure and, eventually, seismic hazard assessment.

On the other hand the report suffers from a number of deficiencies, which are listed below in the order that they occur in the text (first technical and subsequently the principal editorial issues). It is recommended that the editorial issues are addressed in the final version of this deliverable and the technical issues are treated in subsequent deliverables for this task.

Technical remarks and questions:

1. Were the stations installed by BRGM and IGC during the ISARD project used?
2. Quarry blasts: As mentioned above, I think that the use of these ‘ground truth’ events is a strong point of the study. However, how accurately are the locations of these blasts known? From the maps shown the quarries are at least 1 by 1 km so where exactly the blasts were located is important if accuracies better than 1km are desired.
3. Figure 3C: It would be informative to compare the inverted 1D model with the initial 1D model and some independent models (e.g. CRUST1.0).
4. Figure 5: Is the sharp step in Moho depth at about 260km horizontal distance realistic? What would happen if the inversion started with a completely independent 3D model (e.g. CRUST1.0), i.e. how sensitive are the results to the initial 3D model?
5. P. 19: The authors write: ‘The solution is very sensitive to the complete weighting scheme in NNLoc in particular the weighting due to phase picks quality’. Did the authors undertake a sensitivity analysis? This would appear to be necessary given this comment by the authors.
6. Figures 9 to 11: How do these aftershock locations compare to independent locations (e.g. those provided by Renass)? Also how do the aftershock alignments compare to focal mechanisms for these events?
7. Figure 11: These aftershock distributions are quite strange. Were two parallel faults activated in this aftershock sequence? Or is there a timing/location error for some of the stations?
8. Figures 13 and 14: Why are there circles of variations in velocities (like radiating waves), centred on the middle of the map, visible on these figures? This seems strange.
9. Figures 13 to 17: It would be useful to check the resolution of the model by tracing the ray paths and by, for example, undertaking a checkerboard test.

Editorial remarks (only the major problems):

1. Throughout: My principal criticism from an editorial point of view is that the English needs considerable improvement. The poor grammar distracts from the technical content and it is often difficult to understand what the authors mean and actually did. I recommend that the report is proofread by a native English speaker before submitting the final version.

2. Throughout: Similarly to the poor grammar mentioned above, there are: numerous spelling errors, e.g. ‘realize’ (p. 2, ll. 2 and 3 of actual report), ‘sedimentray’ (p. 13, caption of Figure 4 of actual report) and ‘McLaughlin’ (p. 14, l. 17 of actual report), and text formatting issues, e.g. some references given in capital letters while most are not, on p. 21 only the dates for the references are given and not the names of the authors and LaTeX formatting (e.g. dollar signs) included on p. 3 of executive summary. These should be corrected in the final version since they impede understanding and distract the reader. It appears that the report was written in a hurry and insufficient care was taken over the presentation. I recommend that the authors spell check and carefully proofread the report before submitting the final version.
3. Throughout: The commonly-used expression for the procedure to determine the location of earthquakes is ‘localization’. I recommend that this is used by authors rather than ‘location’.
4. Throughout: The authors use the expression ‘plate earth’ when the correct expression is ‘plane Earth’ (or ‘planar Earth’).
5. P. 4 of executive summary and pp. 6-7 of actual report: The details of the data used would be better summarised as a table with columns: network, date range, number of earthquakes, number of stations, number of phases etc.
6. P. 4 of executive summary (and elsewhere): The accelerometers of RAP and BRGM are listed separately even though BRGM runs one of the RAP sub-networks (and OMP the other) in the Pyrenees.
7. Figure 2: Where are the RAP stations on this map?
8. P. 12: The authors state: ‘As previously mentioned, we may remark some discrepancies associated with few Pyrope temporary seismic stations having clock problem [sic]’ but these problems were not mentioned previously in the report.
9. Figure 4 A: It would be useful to add the box and show the same geographical extent as in the other figures (e.g. Figure 4 B). What is the reference for this map?
10. P. 19: I recommend that much of this text is replaced with tables summarising the input parameters. Currently the text is difficult to follow. In general, it is often preferable to summarise input parameters in tables for clarity.
11. P. 20, Inversion algorithm: This section appears to be missing.
12. P. 20, l. 34: What does ‘ $C_1 0^3 + \dots + C_1 0^9 + 1$ ’ mean?
13. P. 28, l. 15: Is there a reference for the statement about the Bouguer anomalies?
14. P. 28, ll. 32-33: These lines appear not to be complete (and there are not comprehensible).

John Douglas

BRGM, Orléans.

16th October 2013

Report on the deliverable D1-89: « **Comprehensive 3D absolute earthquake location (versus 1D) and local seismic tomography of the Pyrenean crust from first arrival times** » by T. Theunissen, S. Chevrot and M. Sylvander (Observatoire Midi Pyrénées). [M. Granet, EOST].

A precise location of earthquakes, including the determination of depth and origin time, is essential for assess the seismic hazard, to identify possible seismic active faults and to build a good data set for local seismic tomography studies. In fact, nowadays, the “mislocation” of hypocenters may be as large as few kilometers (may be 10 or 15 kilometers) on some areas depending on the local geology, the magnitude, the quality of the pickings, the use or not of direct (Pg, Sg), regional phases (Pn, Sn) and reflected phases (PMP), and the network geometry (distribution of the stations with respect to the hypocenter in terms of epicentral distance and of azimuth).

There are different purposes in this work. One of them is to quantify the benefits of a 3D location of local or regional earthquakes – which requires to compute and to use 3D crustal velocity models for both P and S waves – in comparison to a 1D location. The authors announce that a target is the creation of a 3D routine to perform the locations of earthquakes at the Pyrenean seismological center, a goal which I consider, after having read the manuscript, difficult to reach at this step considering the complexity of the processing as it is described, especially since this is still research work. A routine process needs to be based on stable and simple procedures to be run, so that the seismic analyst does not need to "play" with the computer codes and their input parameters.

Overall, the report is dense and accurate, even that sometimes the reader is a bit lost (in the sense where the main aspects are sometimes embedded in a lot of details), leading to some confusion considering the mass of information, the number of velocity models, either a priori model to determine earthquake hypocenters or seismic tomography studies, or final model as a result of the seismic tomography studies. I have been impressed by the quality of the bibliography. On my opinion, for a seismologist working on the question of earthquake locations (which is one of the main tasks of a seismological observatory), we can retrieve in these references the main steps of the state of the art for the last 30 years. I may add that there are a lot of typographical errors and that the quality of figures and of legends is not as good as what one might expect. It looks like the report was not reread before being sent. These needs to be improved.

Before starting to comment on particular points of this report, **I would like to state that the results are only as good as the input data, whatever the algorithms and the quality of the data processing (including the inversion scheme) used are.** That is obvious... The statement given by the authors on page 34 at the end of the report should be seen in that light: “In our case, our dataset is may be insufficient to correctly retrieve a robust 3D model [seismic tomography velocity model] according to the initial velocity in particular in depth”.

Besides the abstract and an executive summary, the deliverables (44 pages including references without abstract and executive summary) are organized in 6 chapters:

- 1. Introduction (about 1 page);
- 2. Geological context (3 pages including a figure showing the main structural units of the Pyrenees);
- 3. Data (3 pages including one figure showing a map of the seismicity [output of the study or from another computations?] and a map of the seismic stations used for the compilation);
- 4. Methodology (11,5 pages including 4 figures: figures 3 to 6);
- 5. Results (13,5 pages including 11 figures : figures 7 to 17);
- 6. Discussion and prospects for this work (1 page).

In the following, I will mainly concentrate on chapters 3, 4 and 5 as the purpose of the work is not to develop on the tectonic aspects.

I- Data.

In order to achieve the objectives (3D absolute earthquake locations, 3D seismic tomography models), this work benefits from a large data set, consisting of different sub-sets:

- Bulletins (phase pickings) from the RSSP (Observatoire Midi Pyrénées - Réseau sismologique de surveillance des Pyrénées): from December 1978 to December 2011, a total of 20 561 earthquakes;
- Manual pickings from the PYROPE and TOPO-IBERIA experiments: from September 2010 to January 2013, a total of 313 earthquakes;
- Bulletins (phase pickings) from the RéNaSS (Réseau national de surveillance sismique, seismic network of the French university and CNRS laboratories) and CEA (Laboratoire de détection géophysique) networks: from December 1987 to February 2013 for RéNaSS and from January 1978 to December 2012 for the CEA network, total number of earthquakes is not found in the report;
- Manual pickings of accelerograms from the RAP (Réseau accélérométrique permanent) et BRGM accelerometric networks: from May 2001 to May 2010, a total of 151 events;
- Data from IGN (Instituto Geográfico Nacional), including IGC (Institut Geològic de Catalunya): from November 1997 to February 2013, a total of 12 469 events.

In addition, the authors added manual pickings obtained from temporary deployments (1996, 1999-2000/2001 and 2006).

One should note that the final data set made of a compilation of these different subsets is not the sum of all data cited above: in fact, many earthquakes were recorded simultaneously by different networks (for example, between the RSSP and IGN/IGC, between the CEA and the RéNaSS...). In addition, some networks use the same seismological stations (for example, RéNaSS and RSSP), but the phase pickings for these stations are not identical because the seismic analyst is different. So, which are the retained arrival times in this work? I think the data from OMP were preferred (if duplicate or triplet or...), but that needs to be clarified and justified.

The data set (events with associated arrival times of local and regional phases) is composed of 22 762 earthquakes for a total of 440 265 arrival times (235 585 P data and 204 860 S data) recorded at 320 seismic stations. In average, there are 10,6 P data (+- 8,6) and 8,3 S data (+- 8,5) per event.

As stated in the beginning, the quality of the data is essential for the quality of the results. Here, the data are clearly heterogeneous: there is a mixing of different data sets obtained for a long period and phase pickings were performed by different seismic analysts on seismograms recorded by different data acquisition systems and different type of seismometers (at least short period and broad band seismometers). I would have expected a detailed discussion on this heterogeneity and on its possible impact on the phase pickings (the arrival times are the basic data) due to this heterogeneity.

For example, one can calculate and discuss the hodochrones for the direct and refracted phases for each data set, and then globally. Another way is to show the histograms of the residuals which result from the routinely preliminary location of earthquakes (using HYPO71 or another code)... **The point is "to show the data"** so that the reader may have a better idea of their quality. I would also suggest

to provide histograms of the “gap” (azimuthal range without data) for the whole set of the initial catalog (the 3D location will not change fundamentally this “indicator”).

II- Methodology

The manuscript described in detail the methodology which follows four steps. The approach is the following: after obtaining the "best" earthquake hypocenters for the entire seismicity (see above concerning the data set), and the associated upper crust velocity model (I shall come back to this point later), the lower crust has been imaged by using refracted waves. One objective is to test the 3D seismic tomography sensitivity to the initial velocity model. These successive steps are:

- Initial velocity model determination: inversion of a 1D minimum model (which appears at the end as the “best” one for the location of earthquakes) and associated station delays;
- 3D earthquake locations within the initial a priori velocity models using station delays (1D minimum velocity models and other 3D a priori models);
- 3D local seismic tomography using Pg and Sg phases, and final earthquake locations;
- 3D local seismic tomography using all direct (Pg, Sg) and refracted (Pn, Sn) first arrivals – there is no information in the manuscript about PMP and a possible misinterpretation between Pn and PMP – combining 3D a priori models including results from upper crust seismic tomography, Moho information and final earthquake locations.

At the end of the successive steps, four velocity models are computed:

- Minimum 1D models with associated station delays; flat and ellipsoidal earth approximation are considered: these models are used for earthquake locations. The 1D minimum velocity model is obtained from the VELEST program (developed by E. Kissling, 1988, 1994, 1995). This program can also be used to jointly determine a 1D velocity model, hypocenters and station delays using P and S arrival times. A reduced data set is used in the study (2 051 events having *at least - do I understand well?* - 12 P and 6 S with a gap less than 180°). In order to jointly determine the upper layers velocity fields, the hypocenters position and the stations correction, only Pg and Sg phases are retained. Refracted phases are added in a second step to describe the lower layers and to calculate the station corrections for the distant stations. One should note that during this second step, the previously determined upper layers model and hypocenters position are damped (does that mean that the values of these parameters are fixed? This is not clear). The use of station delays is underlined by the authors: with station delays, which goal is to limit the bias introduced by velocity anomalies situated just beneath the stations, the earthquake location is improved.
- A P-minimum 1D model together with a constant Vp/Vs ratio of 1,73 and a fixed Moho depth at 35 km depth: this model is used for initial velocity model in tomography;
- A P-minimum 1D model together with a constant Vp/Vs ratio of 1,73 and a smooth Moho depth (obtained from a compilation of seismic experiments and receiver function calculation): this model is used for initial velocity model in seismic tomography;
- A 3D a priori model with the ellipsoidal earth approximation: this model is used for earthquake locations purpose and for initial velocity model in tomography.

3D a priori models are built through the combination of many consecutives 2D lines equally spaced. To do that, 4 interfaces are realized: relief topography and bathymetry; basement top; lower crust limit; Moho topographies of Iberia and Eurasia crusts.

The locations of earthquakes are determined by using the NonLinLoc (NLL) code by Lomax et al. (2000) for 3 reasons: (i) the solution is described by a probability density function based on Equal

Differential Time (EDT) – one advantage is that the origin time is determined independently of the spatial position (there is a trade-off between the Z (depth) spatial position and the origin time); (ii) the weighting scheme is well designed; (iii) the search algorithm allows well to browse the entire structure, thus leading to a good estimate of the location. The travel times calculations are based on the Eikonal propagation equation. I find all these “options” well adapted.

I just would like to mention that the question of the weighting scheme is extremely complex. In the NLL code, the weighting scheme considers a station-distance weighting to each travel-time and a weight for each station that is a function of the average distance between all stations used for the location. I am personally not really convinced that this “*helps to correct for irregular station distribution and limits correlated travel-times errors*” (a sentence from the report). Such a weighting is used since a long time for routine processing in many observatories. Therefore again: there is no data processing which can correct for poor network geometry with respect to the earthquakes locations. One of them, the simplest, is a weighting scheme by quadrant (an azimuthal range of 90°). It should be added that the parameterization of the NLL code also requires to carefully consider the values attributed to travel-time errors (here, 5 % of the travel-time of seismic waves with a minimum of 0.05s and a maximum of 2s: why is that choice?) and for phase picks quality (here, 0, 1, 2, 3 and 4, respectively for errors 0.05, 0.2, 0.3, 0.5 and 4s). The manuscript gives no information on the reasons for such a weighting. The question is to know if all the arrival times were carefully reexamined, implying that the authors had again a look at the seismograms? The answer is probably no. The authors state that the solution is very sensitive to the complete weighting scheme (yes, of course), but do not comment any further on that.

In order to valid the method, a selection of events is used as a reference: three sequences of seismic events recorded by a temporary network after a main event (Argelès-Gazost, 2006; Causerets sequence, 2002; Agly sequence, 1996) and three quarry blasts (for which the location is exactly known). These sequences are used to check: a) the clustering of the seismicity by the “absolute” earthquake locations process; b) network criteria depending on the velocity model. In fact, many tests were performed to check various velocity models with or without station corrections, and the values of some parameters.

Concerning the 3D local earthquake seismic tomography, the authors used a method which inverts simultaneously for the velocity distribution and the hypocenters from the first arrival times of direct and refracted phases. This is a classical approach since Aki and Lee (1976), which has been used in many different tectonic contexts. The code has been developed by Monteiller et al. (2005). I have no specific comments on the inversion scheme itself which is realized by the LSQR algorithm (due to the large amount of data and unknowns?) and which integrates a classical regularization (weighting, smoothing and damping). The regularization process during the inversion scheme is achieved thanks to the adjustments of a lot of different parameters. The authors say that “these parameters are fixed during the inversion and are defined after multiple tests in order to obtain the best compromise between variance reduction, smoothing and amplitude anomalies”. From my own experience, this is not so obvious. Hence, the reader needs additional information (with the help of tables or figures) to have a better understanding on the selection criteria of parameters (for example, the damping or the weighting have a strong influence on the final perturbations values).

The region under study is modeled by a regular small grid (4 x 4 x 2 km³). Except misreading on my part, I have not read in the document the total number of unknowns of the tomographic problem.

There is a confusing number of “velocity models” used in this manuscript (1D, 3D, a priori or final, with or without station delays, with an earth ellipsoidal approximation or not...) so that the reader is

sometimes lost... I would suggest to present a table which lists and describes each velocity model, and gives few words on their use.

III- Results

III-1. Initial earthquake locations

Tests are made by using the 1D VELEST and the 3D a priori models (flat earth approximation is tested only on the 1D VELEST and station corrections are tested on both the 1D and the 3D models: station corrections are estimated from an average of residuals obtained on a subset of data and the 3D a priori velocity model). Results are compared with the ones obtained from the HYPO71 code (an average from few runs with different initial depths). The initial earthquake locations are tested thanks to the reference events defined above. A so-called "optimal solution" is obtained from events (subset of the Argelès, Causerets and Agly sequences) which were recorded by at least 10 stations with Pg and Sg phases. There are no specific comments on this procedure.

The main results are:

- Using the station corrections greatly improve the earthquake absolute location for 2 quarry blasts;
- Using ellipsoidal earth approximation improves the depth determination in all cases;
- Earthquake absolute location within the 3D a priori model based on the NLL code is quite bad: there are errors of 2km horizontally and 3 km vertically (one should note that these errors decrease when computations are made without S phases and without station corrections).

These tests are illustrated on figures (7 and 8: results of absolute quarry blasts location; 9, 10 and 11; 12: results of synthetic absolute earthquake locations for the well located 20th February 1996 event from the Agly sequence within the 3D tomography model). The figures are in general not easy to read and need to be improved.

In fact, results are mainly presented in a visual form and conclusions are not so easy to derive. One point is that earthquake locations obtained from the 1D VELEST minimum velocity model seem to be the best ones (again, this is based on only visual criteria). That is why I suggest to define (and to compute) a set of criteria to quantitatively measure the mislocation (if it exists). This includes equally the need to measure the (expected) improvement of the hypocenter locations relative to those obtained by the HYPO71 code (which must be used with a good initial velocity model).

III-2. Upper crust model

Two models are calculated, one by using the 1D VELEST initial model, the second from the 3D a priori velocity model (see figures 13 and 14: the (colour) scales are too small). This upper crust model is obtained by fixing the hypocenters and by using only Pg and Sg phases (and epicentral distances less than 121 km... **This suggests that only Pg and Sg are recorded to distances smaller than 121 km, but only computations of the hodochrones could valid this).**

While the 1D VELEST initial velocity model leads to a better variance reduction (which also depends on the quality of the data set), is on the other hand the best RMS obtained with the 3D a priori model. I have no specific comments on the tomography models itself (in the discussion section, the authors refer to a positive Bouguer anomaly which is not shown on the figure!). The earthquake locations have not been tested within these two models.

I have no specific comments on the tomography pictures, except that one observes large Vp values along the chain for the 1D VELEST initial velocity model. Moreover, this is underlined by the authors.

III-3. Crust model

Results are shown on the figures 15, 16 and 17. The crust models are calculated by fixing the initial hypocenter and by using all direct and refracted phases (quite normal!). The initial velocity models are the ones obtained for the upper crust. Why don't also use a lower crust initial velocity model? During the process, the origin time and the hypocenter position are fixed (hence, data are used only to constrain the final velocity model). Two results are underlined: i) the use of a 2D smooth a priori Moho interface seems to improve the results of inversion; ii) the crustal root, west of the Pyrenees, is partially recovered when using a Moho at 35 km depth.

I have no specific comments on the tomography models.

Main conclusions:

- The presented report is a difficult but necessary work in order to improve significantly the location of earthquakes in complex tectonic areas (for example, for seismic hazards studies) and to calculate high spatial resolution 3D images of the crust; the work is well advanced, but it still needs substantial improvements (also in the writing and the quality of figures).
- The data are heterogeneous (different data sets are merged). The authors should take more care to present and discuss these data so that the reader can get a good idea of this heterogeneity. For example, I would like to see hodochrones. Without good data, no good models can be expected!
- The algorithms used seem - from my point of view - adequate and well mastered. However, there is clearly a lack of a quantitative discussion on the choice of certain parameters (damping, weighting ...) that strongly impact on the final earthquake locations and hence the tomographic model.
- It misses a quantitative estimate of the improvement made by the new models compared to the results obtained with HYPO71.
- The suggestions for future developments seem appropriate.